ALL-STOKES SINGLE DISH DATA with the RHSTK (Robishaw/Heiles SToKes) SOFTWARE PACKAGE
June 26, 2017

Carl Heiles[1], Tim Robishaw[2], Amanda Kepley[3], & Furea Kiuchi[4]

[1] *Department of Astronomy, UC Berkeley, B-20 Hearst Field Annex, Berkeley, CA 94720, USA; heiles@astro.berkeley.edu*

[2] *Covington Fellow, National Research Council, Herzberg Institute of Astrophysics, DRAO, Penticton, BC V2A 6J9, Canada; tim.robishaw@nrc-cnrc.gc.ca*

[3] *NRAO, Green Bank, W. Va., 24944, USA; akepley@nrao.edu*

[4] *Department of Physics and Astronomy, University of Kentucky, Lexington, KY 40506, USA; kiuchi@pa.uky.edu*

June 26, 2017

ABSTRACT

We discuss practical aspects of all-Stokes spectropolarimetric calibration for single-dish radio telescopes using digital spectrometers that produce auto- and cross-correlation products. We describe our polarization-related software package, which we call Robishaw/Heiles SToKes (RHSTK), and provide examples for reducing position- and frequency-switched data, deriving magnetic fields from Zeeman-splitting data, and for deriving Mueller matrices and polarized beam properties. We describe how to run it in the GBTIDL environment. We don't explicitly use RHSTK at Arecibo, but nevertheless we describe our reduction procedures at Arecibo.

We begin with the basics—theory and practice—in §1. We describe the quagmire of standards and conventions for polarization, and even magnetic field direction, in §2. We then attempt to describe how to use RHSTK for calibrating astronomical data, when the system's Mueller matrices are known, in §3 and §4. §5 describes how to determine the system's Mueller matrices by observing standard polarization calibration sources. Finally, §7 and §8 describe the application of RHSTK to GBT and Arecibo data.

Contents

1.   BASIC CONCEPTS, DEFINITIONS, AND CALIBRATION PARAMETERS

1.1.   The Process of All-Stokes Calibration

1.1.1.   All-Stokes Calibration in a Nutshell

Figure 1 is a block diagram showing a telescope with two signal paths, one for each polarization, labeled 'X' and 'Y'. These might be either approximately orthogonal linear polarizations or circular polarizations. The essence of all-Stokes observing is to measure the time-average autocorrelation-products XX and YY together with the cross correlation products XY and YX. Correlation products are functions of time delay, and self-products are always symmetric with respect to the sign of the time delay. In contrast, cross-products have arbitrary symmetry, and here we denote the symmetric portion by XY and the antisymmetric portion by YX. Thus, we measure four different correlation functions.
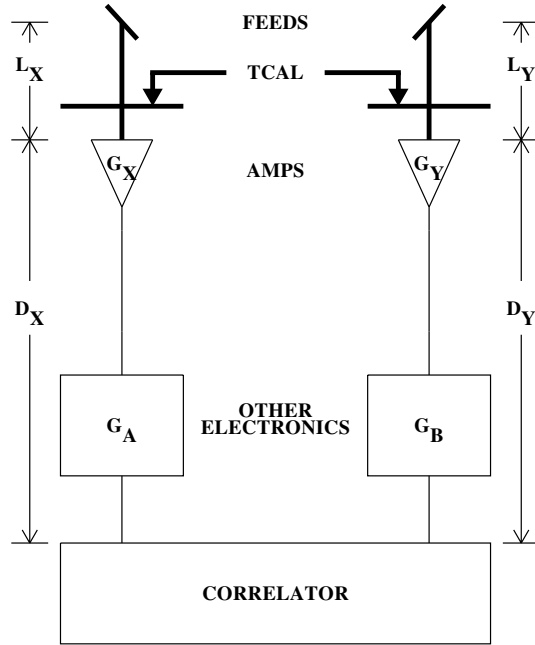
Fig. 1.— Block diagram of a dual-polarized single-dish radio telescope. Thick lines represent time-independent aspects, which are calibrated by the feed's Mueller matrix. Thin lines represent time-variable aspects, which are calibrated frequently using the Noise Diode: the r.f. amplifier gains (G_X, G_Y), the 'other electronics' gains (G_A, G_B), and the delays caused by cable length and electronics represented by the lengths (L_X, L_Y); all of these quantities are time-variable. This diagram implies there is zero coupling (crosstalk) between the two signal paths, which is not the case in real life; crosstalk is represented in the feed's Mueller matrix.

These correlation functions are provided by the Correlator, shown in Figure 1. They are calculated digitally and refer to the signals presented to the correlator input. The correlator inputs differ from the astronomical electromagnetic waves because they have gone through the telescope

system, which includes the feed, electronics, and cables. Inside the correlator, these analog signals are digitized.

We are interested in the astronomical signals, so we need to remove the effects of the telescope system. In other words, we need to calibrate the measured correlation products and turn them into the four Stokes parameters. This calibration process uses

1. A standard noise source called the 'Noise Diode' whose intensity is known and constant, and whose relative phase injected into the two polarization channels is not necessarily known but is constant in time. We measure the Diode deflection (DIODEON – DIODEOFF) with the correlator, which tells us the gains and relative phase of the thin lines in Figure 1, which is the telescope system after the point where the Diode is injected .

2. Applying a Mueller matrix that corrects for the thick lines in Figure 1, which is the telescope system before the Diode is injected. This includes imperfections of the feed and the path length difference $L_X - L_Y$.

Applying these corrections provides the desired astronomical Stokes parameters in Kelvins.

1.1.2. More Detail: Time-Independent and Time-Dependent Aspects of Calibration

The power in each path is the voltage squared, which we denote by XX or YY, and we call these 'self-products'. This diagram implies there is zero coupling between the two signal paths, which is not the case in real life. We account for this coupling in the feed's Mueller matrix, which is discussed in §1.5.3.

We regard the thick-line portion of Figure 1 as *constant in time*; this part is embodied in the feed's Mueller Matrix $\mathbf{M_{feed}}$ (§1.5.3). This portion includes the feed and Noise Diode circuitry. These components are mechanical structures and don't change without good reason. What's important for *polarimetry* are the *dimensions and cable lengths*, so even if the Noise Diode itself is replaced without changing cables, the thick-line portion remains unchanged for polarimetry. Of course, a different Noise Diode will produce different noise power, which changes the overall intensity calibration, but not the polarization calibration. An astronomical observer is usually given the Diode strength in Kelvin, which is its equivalent antenna temperature, and one normally assumes it to be reliable and constant with time; this is usually a good approximation.

The thin-line portion of Figure 1 is *time-variable*. Consider the relative phase of the two signal paths. This depends on at least two things: the cable length difference and the phase delays produced by active circuit elements such as amplifiers. The cables can be very long (measured in hundreds of meters at Arecibo, and thousands at the GBT), so thermal expansion plays a role in their lengths; moreover, there is no guarantee that individual cables used for each signal path don't happen to get interchanged, either by a technician or by automatic assignments of optical fibers by the system. The gain and phase delay of an amplifier depend on applied voltages and temperature, and moreover an individual amplifier usually produces a 180° phase jump; the number of amplifiers can change as gains are automatically adjusted.

1.2.   The Power Gains of X and Y Signal Paths

Most observers are not concerned with polarization information, so they treat the X and Y signal paths independently. They turn on and off the Diode and measure its deflection in terms of correlator counts; knowing the Diode's strength in Kelvin, this provides the 'Counts per Kelvin', which we call CpK. This is a power gain, not a voltage gain; that is, CpK relates the equivalent system temperatures to the counts of the self-products XX and YY. The numerical value of CpK for each signal path depends on the electronics, in particular the gains of the amplifiers in the chain (G_X and G_A for the X-path in Figure 1). Being active elements, some of which are cryogenically cooled, these gains cannot be considered constant with time, and they are calibrated at intervals that may be separated by order of minutes. The calibration procedure uses the Diode deflection, i.e., the comparison of DIODEON and DIODEOFF measurements made close in time.

The gain, i.e. CpK, is a very strong function of frequency within the observing band. Band-limiting filters define the spectral bandpass that enters the digital spectrometer, and their gains vary between almost zero and the maximum within the bandpass. The black and magenta curves of Figure 2 show typical examples (top left panel for Arecibo's Interim Correlator, top right for the GBT's Spectral Processor). We characterize this frequency-dependent gain by two concepts. One is a representative value of CpK over the bandpass, and the other is the 'bandpass shape'. We define the former by averaging over a specified spectral channel range in the output spectrum, which normally includes most of the bandpass except for the ends.

1.3.   The Relative Phase Delay Between X and Y Signal Paths

To derive polarization, we must measure the cross-correlation of the X and Y signals. This cross-correlation depends not only on the above-defined gains, but also on their relative phase delay. We need to use the Diode for calibrating the phase difference, because some of its components can be time-variable. If each signal path has its own Diode, so that the X and Y Diode voltages are uncorrelated, then the XY product for the Diode deflection is zero, so we cannot measure the relative phase delay. However, we arrange that the Diode deflections are correlated. To accomplish this, one can use a single Noise Diode and a power splitter (as is done at the GBT and Arecibo); or one can insert the noise in the feed, or at the paraboloid's vertex (as was done with the Hat Creek 85-footer), to provide full correlation (for example, in the case of native linear feeds, by radiating the Diode's power with a probe at 45° to the orthogonal X and Y probes).

The relative phase of the X and Y Diode deflections depends on, at minimum, the following factors. The first is constant in time and, consequently, is embodied in the Mueller Matrix correction; the others are calibrated concurrently by fitting a linear phase gradient with frequency.

1. The phase difference between the correlated Diodes as seen by the two first amplifiers. If the Diode is injected with a waveguide probe or vertex radiator, this phase difference should depend only on the length difference of the cables that connect the feed to the amplifiers. If it is injected by cables, using a power splitter and directional couplers, then this phase difference also results from cable length differences in the cables connecting the Diode to the two feeds, and in addition there might be a phase offset introduced by the power splitter and directional couplers. As depicted by the thick lines in Figure 1, this component of phase offset depends on mechanical structures and should be stable and constant with time.

2. The phase difference introduced by the different cable lengths D_X and D_Y, which can be time-variable because the cables are long and environmental conditions (temperature) come into play, as mentioned above. The relative phase delay ψ from the cable length difference $\Delta D = D_Y - D_X$ varies linearly with frequency:

$$\frac{d\psi}{df} = \frac{2\pi\,\Delta D}{v_{ph}}\,, \tag{1}$$

where v_{ph} is the phase velocity in the cable. Typical values at both Arecibo and GBT are a few tenths of a radian per MHz, which leads to $\Delta D \sim$ several meters.

3. The phase difference introduced by components in the X and Y signal paths. Some of these are active circuit elements and can change with time.

4. The signal entering the digital spectrometer must pass through a band-limiting filter. Particularly for the GBT, these filters have steep gain changes with frequency. This automatically introduces phase delays, the minimum values of which can be calculated from the Kramers-Kronig relations. The exact formula for electrical circuits is equation (2) of Bode (1940)[1]:

$$[Phase\ Shift](f_c) = -\frac{1}{\pi}\int_{-\infty}^{\infty}\frac{dG}{du}\,\ln\left[\coth\left(\frac{|u|}{2}\right)\right]du\,, \tag{2}$$

where G is the filter power gain in Nepers relative to an arbitrary reference, f is frequency, and $u = \ln\left(\frac{f}{f_c}\right)$. The weighting function $\ln\left[\coth\left(\frac{|u|}{2}\right)\right]$ is sharply peaked at $f = f_c$, so a good approximation eliminates the integral and uses only the local derivative (equation 22 of O'Donnell, Jaynes, & Miller 1981)

$$[Phase\ Shift](f_c) = -\frac{\pi}{2}\frac{dG}{du}\bigg|_{u=0}\,. \tag{3}$$

(Note that $u = 0$ corresponds to $f = f_c$). Thus a non-flat filter produces phase shifts.

Our work at Arecibo has been done with the interim correlator, for which the baseband low-pass filters are digitally defined and are remarkably flat; Figure 2, left-hand panel, shows the positive-frequency half of the X and Y signal-path filters for bandwidth 12.5 MHz (cutoff frequency 6.25 MHz). Phase shifts occur only at the end, where the response of filters drops precipitously.

In contrast, the GBT Spectral Processor filters are far from flat. For example, the 0.625 MHz bandwidth filter is shown in the right-hand panel of Figure 2. The phase difference between the X and Y signal paths is the cyan line in the bottom half, and there is a visually perceptible phase delay difference of a *very* approximate ~ 0.2 radians across the band. When reducing real phase-calibration data, our software derives a phase slope ~ 0.24 rad MHz^{-1}, which would produce a total change of ~ 0.12 radians across the band. It seems that at least some of the phase slope arises from the difference between the X and Y filters. Clearly, to the extent that the filters in the X and Y signal paths are identical, the relative phase delay cancels out.

---

[1]You would miss a lot if you pass up the opportunity to read this paper, particularly the first six pages. Go to `http://www.alcatel-lucent.com/bstj/`.
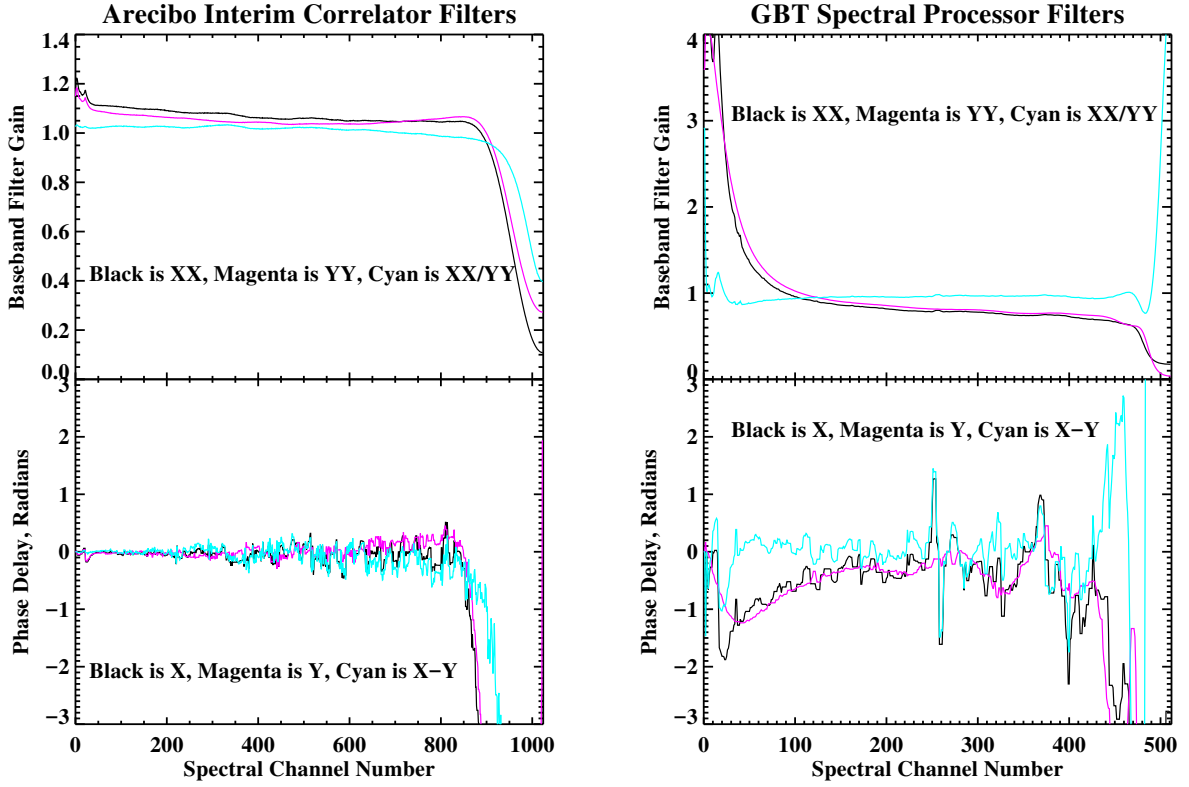
Fig. 2.— Filter shapes and their theoretical phase delays for the Arecibo Interim Correlator (left panel) and the GBT Spectral Processor (right panel).

1.4. The Cross Products: Symmetrical and Antisymmetrical, Real and Imaginary

Above, we introduced the self-products XX and YY. The cross-products XY and YX are the essential additional measurements required to obtain all four Stokes parameters. Let's compare auto-correlation (XX) and cross-correlation (XY) products.

First, consider the auto-correlation product XX. Written as an integral, we speak of the auto-correlation function $A(\tau)$, which is a function of time delay τ. Disregarding niceties such as limits of the integral, it's defined as

$$A(\tau) = \int X(t)X(t+\tau)dt \,. \tag{4}$$

Clearly, it's symmetric with respect to positive and negative τ. Moreover, it must peak at $\tau = 0$, because a signal cannot be more perfectly correlated than with itself with no time delay. We then derive the power spectrum $XX(f)$ by taking the Fourier Transform (FT), taking advantage of the fundamental relation $XX(f) = FT(A(\tau))$. Because $A(\tau)$ is Real and symmetric, $XX(f)$ is symmetric and its Imaginary component is zero.

Next, consider the cross-correlation product XY. Written as an integral, we speak of the cross-correlation function $C(\tau)$, which is a function of time delay τ. Disregarding niceties such as limits of the integral, it's defined as

$$C(\tau) = \int X(t)Y(t+\tau)dt \,. \tag{5}$$

Clearly, $C(\tau)$ is *not necessarily symmetric* with respect to positive and negative τ, because X and

Y are different signals. Moreover, there is no reason for it to peak at $\tau = 0$. We derive the cross-power spectrum $XY(f)$ by taking the Fourier Transform (FT). Because $C(\tau)$ is Real, but *not* symmetric with respect to τ, $XY(f)$ is not symmetric and, in particular, its Imaginary part is *nonzero*. In other words, $XY(f)$ is Complex. More narrowly, it has Hermitian symmetry: its Real part is symmetric and its Imaginary part is antisymmetric with respect to f. Suppose, for example, that X and Y are perfectly correlated, but have a 90° phase shift. Then $Re(XY(f))$ is zero.

Thus, we can speak of the Real and Imaginary parts of $XY(f)$. In the rest of this document, we use the shorthand notation

$$XY \equiv Re(XY(f)) \tag{6a}$$

$$YX \equiv Im(XY(f)) \tag{6b}$$

1.5. Stokes Vectors and their Transformations in the Measurement Process

We need to turn these self- and cross-products into the four calibrated Stokes parameters. The Stokes parameters depend on the reference framework and definitions. Here, by 'calibrated Stokes parameters', we mean specifically that they are defined as in conventional astronomical usage: **(1)** the position angle of linear polarization increases from North towards the East, and (**2**) the sign of the circularly polarized Stokes V is correct. In contrast, the system's Stokes parameters do not necessarily follow any, or all, of these conventions. Thus, we need to convert the system's Stokes parameters to the astronomically-defined ones. We accomplish this by applying a series of transformations. These transformations are best accomplished by considering the four Stokes parameters as the Stokes vector and applying matrix techniques; the matrices are called Mueller matrices. We can regard the Mueller matrix as the transfer function associated with an individual device or operation, or a set of them.

We begin by writing the four Stokes parameters as the Stokes vector

$$\mathbf{S} = \begin{bmatrix} I \\ Q \\ U \\ V \end{bmatrix}. \tag{7}$$

1.5.1.   Using $\mathbf{M_{feed}}$ and $\mathbf{M}_\rho$ to Relate $\mathbf{S}_{\rho=0}$ to $\mathbf{S}_{\mathrm{obs}}$

On its voyage from the source to the output of the correlator, the source's electromagnetic radiation encounters the following transformations, in the following order:

1. As a source is tracked with an alt/az mount, the feed rotates on the sky and interchanges power between the two linearly-polarized Stokes parameters Q and U. We define $\mathbf{S}_{\rho=0}$ as the Stokes parameters seen by the feed at parallactic angle zero. $\mathbf{S}_{\rho=0}$ is not necessarily equal to the Stokes vector of the source $\mathbf{S}_{\mathrm{src}}$ because of the mechanical mounting of the feed; we account for this with $\mathbf{M_{astron}}$ below, where we define $\mathbf{S}_{\rho=0} = \mathbf{M}_{\mathrm{astron}}^{-1} \cdot \mathbf{S}_{\mathrm{src}}$. Then as the telescope tracks the source and ρ is nonzero, the Stokes vector incident on the feed is

$$\mathbf{S}_\rho = \mathbf{M}_\rho \cdot \mathbf{S}_{\rho=0} = \mathbf{M}_\rho \cdot \mathbf{M}_{\mathrm{astron}}^{-1} \cdot \mathbf{S}_{\mathrm{src}}. \tag{8}$$

$\mathbf{M}_\rho$ is a simple rotation matrix for Stokes Q and U:

$$\mathbf{M}_\rho = \begin{bmatrix} 1 & 0 & 0 & 0 \\ 0 & \cos(2\rho) & \sin(2\rho) & 0 \\ 0 & -\sin(2\rho) & \cos(2\rho) & 0 \\ 0 & 0 & 0 & 1 \end{bmatrix}. \tag{9}$$

2. $\mathbf{M_{feed}}$ specifies the relationship between $\mathbf{S}_\rho$, which enters the feed, and the feed output. The feed output is corrected for the rest of the electronics chain by the Noise Diode signal as discussed in §4.1, so we can consider the feed output as the *observed* Stokes vector $\mathbf{S}_{\mathrm{obs}}$. The feed's transfer function for the astronomical signal $\mathbf{M_{feed}}$ is measured relative to that of the Noise Diode. We measure $\mathbf{M_{feed}}$ itself using the procedures in §5 and §6; the details are discussed by Heiles et al. (2001b). So we can write

$$\mathbf{S}_{\mathrm{obs}} = \mathbf{M_{feed}} \cdot \mathbf{S}_\rho = \mathbf{M_{feed}} \cdot \mathbf{M}_\rho \cdot \mathbf{S}_{\rho=0}, \tag{10}$$

3. The 'astronomical' Mueller matrix $\mathbf{M_{astron}}$ specifies the relationship between the telescope's Stokes parameter definitions and the conventional astronomical definitions. Specifically, it accounts for three things:

   (a) The angle of the X and Y E-field probes in the feed with respect to the mechanical axes of the telescope.

   (b) The handedness of the position angle of linear polarization. Specifically, Stokes Q or U must be multiplied by -1 if the position angle 'rotates the wrong way'.

   (c) The sense of circular polarization, i.e., the sign of Stokes V.

In equation 8, the incoming Stokes vector $\mathbf{S}_{\rho=0}$ is defined relative to the angle at which the feed's X and Y E-field probes are mounted relative to the telescope axes. For example, if the X and Y probes are parallel and perpendicular to the telescope's azimuth and altitude axes, then Q_{obs} indicates the difference in power between these two axis orientations; in contrast, if the feed is mechanically mounted so that the X and Y probes are at $\pm 45°$ to the telescope's axes, then it's U_{obs}, not Q_{obs}, that indicates the difference in power between the two axis orientations. Similarly, the system's response to circular polarization, Stokes V, depends on whether X or Y is regarded as the Imaginary input to the Fourier transform.

Thus, we define $\mathbf{M_{astron}}$ so that, when it is applied to $\mathbf{S}_{\rho=0}$, we obtain the astronomically-defined Stokes parameters for the observed source $\mathbf{S}_{\mathrm{src}}$, i.e.,

$$\mathbf{S}_{\mathrm{src}} = \mathbf{M_{astron}} \cdot \mathbf{S}_{\rho=0}. \tag{11}$$

Generally, $\mathbf{M_{astron}}$ looks like $\mathbf{M}_\rho$ in equation 9: it consists of a 2×2 rotation matrix in the inner four elements, which expresses the mechanical mounting angle of the feed on the telescope structure; and a ± 1 in the bottom right element to account for the definition of Stokes V. For example, for the GBT 1–2 GHz receiver, the telescope's sense of circular polarization, Stokes V, happens to match the IAU definition (which is $R - L$, where R and L satisfy the IEEE definition of circular polarization—R means clockwise rotation of the electric field as viewed by the transmitter); and the mechanical mounting angle of the X and Y probes is $45°$ with respect to the telescope's azimuth and elevation axes. Thus, for that

receiver, we have

$$\mathbf{M_{astron}} = \begin{bmatrix} 1 & 0 & 0 & 0 \\ 0 & 0 & 1 & 0 \\ 0 & -1 & 0 & 0 \\ 0 & 0 & 0 & 1 \end{bmatrix} . \tag{12}$$

1.5.2. Obtaining the Holy Grail, $\mathbf{S}_{\mathrm{src}}$

With all of the above, we have the final succinct result: the relation between the observed Stokes vector $\mathbf{S}_{\mathrm{obs}}$ and the source Stokes vector is $\mathbf{S}_{\mathrm{src}}$ is

$$\mathbf{S}_{\mathrm{src}} = \mathbf{M_{astron}} \cdot (\mathbf{M}_{\mathrm{feed}} \cdot \mathbf{M}_\rho)^{-1} \cdot \mathbf{S}_{\mathrm{obs}} . \tag{13}$$

1.5.3. Turning Calibrated [XX, YY, XY, YX] into Mueller-Corrected Stokes Parameters [I, Q, U, V]

Suppose we have derived properly calibrated self-products (XX, YY) and cross-products (XY, YX) by following the procedures in §4.1 below. That is, the powers are expressed in Kelvins and the instrumental phase between X and Y has been removed. These statements imply that (1) all time-variable effects—the thin-line portions of Figure 1—have been eliminated by using the Noise Diode, and (2) the bandpass effects have been accounted for.

Suppose, further, that the feed's polarization is native linear and that there are no imperfections. Then $\mathbf{M}_{\mathrm{feed}}$ would be diagonal and the relationship between the voltage products and the observed Stokes vector $\mathbf{S}_{\mathrm{obs}}$ would be

$$\mathbf{S}_{\mathrm{obs}} = \begin{bmatrix} I_{\mathrm{obs}} \\ Q_{\mathrm{obs}} \\ U_{\mathrm{obs}} \\ V_{\mathrm{obs}} \end{bmatrix} = \begin{bmatrix} XX_{\mathrm{obs}} + YY_{\mathrm{obs}} \\ XX_{\mathrm{obs}} - YY_{\mathrm{obs}} \\ 2XY_{\mathrm{obs}} \\ \pm 2YX_{\mathrm{obs}} \end{bmatrix} . \tag{14}$$

Similarly, for native circular, we would have

$$\mathbf{S}_{\mathrm{obs}} = \begin{bmatrix} I_{\mathrm{obs}} \\ Q_{\mathrm{obs}} \\ U_{\mathrm{obs}} \\ V_{\mathrm{obs}} \end{bmatrix} = \begin{bmatrix} RR_{\mathrm{obs}} + LL_{\mathrm{obs}} \\ \pm 2LR_{\mathrm{obs}} \\ 2RL_{\mathrm{obs}} \\ RR_{\mathrm{obs}} - LL_{\mathrm{obs}} \end{bmatrix} . \tag{15}$$

The sign ambiguities above arises because one can't be sure how the native polarizations are treated inside the correlator. Resolving these sign ambiguities is part of the calibration process and is embodied in $\mathbf{M_{astron}}$.

1.6. ¡¡¡Important Comment on Mueller Correcting for Native Linear Polarization!!!

For native linear polarization, the measured Stokes $Q_{\mathrm{obs}} = XX - YY$ and is the difference between two large numbers. The XX and YY spectra have independent gain calibrations which are not perfect, for three reasons: (1) the DIODEON/DIODEOFF deflection has some noise; (2)

the assumed Diode values are not perfect, and the actual ones certainly depend on frequency and might even depend on time; and (3) the X and Y receiver gains almost certainly change a little with time while observing after the intensity calibration was performed. Thus, for native linear polarization, the Q_{obs} *is not accurate*. However, the U_{obs} *is* accurate because it is determined by the cross-product XY, for which gain uncertainties and fluctuations are unimportant.

When you correct for parallactic angle by applying $\mathbf{M}_\rho$ as in equation 10, you apply a rotation matrix to obtain the *source* Stokes parameters $(Q_{\mathrm{src}}, U_{\mathrm{src}})$ from the *measured* ones $(Q_{\mathrm{obs}}, U_{\mathrm{obs}})$. This means that *both Q_{src} and U_{src} contain the *inaccurately measured Q_{obs}. Accordingly, when Mueller-correcting native linear polarizations, you might well do better by *not* correcting for parallactic angle. You can then do a least-squares fit of the parallactic angle variation of the accurately-measured U_{obs} using equations 8 and 9 to derive *both Q_{src} and U_{src} (!).

We illustrate this technique in the `pswitch` example (see §4.4.2). Clearly, applying this fitting technique requires having a considerable range in observed parallactic angle[2]—so you have to plan ahead *before* observing.

1.7. ¡¡¡Important Comment on Observing 21-cm Line Zeeman Splitting!!!

At the GBT, the L-band system (1-2 GHz) uses the secondary focus. There are severe sidelobes, particularly from spillover around the secondary reflector, and because the Galactic 21-cm line exists everywhere on the sky, these sidelobes always see it. This contaminates the measured 21-cm line spectra. Robishaw & Heiles (2009) developed an approximate model of these sidelobes. They found three components: (1) spillover around the secondary reflector, which is the most serious; (2) a component caused by reflection from the screen, which is located near the secondary; and (3) the Arago spot.[3]

The sidelobes are strongly polarized in an unknown and unmeasurable way, so whenever the contribution to I is large, the contribution to V is probably also large. *This polarized sidelobe contamination is the limiting factor for Galactic 21-cm line Zeeman splitting results!* Robishaw & Heiles wrote an IDL procedure called `predict_gbt_sidelobes_rhstk` to estimate the sidelobe contributions for Stokes I, which is available in the RHSTK package (§7.1). We show an illustrative example of its use in the frequency-switched example (§4.4.1).

2. STANDARDS AND SIGN CONVENTIONS: A BIG MESS

The magnificent review of the Zeeman-splitting literature of radio astronomy by Robishaw (2008) makes clear the rampant confusion regarding definitions and signs of Stokes V and the derived magnetic fields. Accordingly, we provide here a very brief summary.

The International Astronomical Union has adopted definitions for the two circular polarizations and, also, Stokes V (IAU 1974). The IAU definitions for the polarizations follow the IEEE definitions, which are opposite to those conventionally used by physicists. The IEEE definition of

---

[2]To calculate parallactic angle, use our routine `parangle.pro`, which is available in the RHSTK package.

[3]After Robishaw & Heiles (2009) appeared, the NRAO staff published a more detailed and accurate model of the sidelobes; see Boothroyd et al. (2011).

RCP is: as viewed from the transmitter, the E-vector rotates clockwise. The IAU definition of Stokes V is: $V = \mathrm{RCP} - \mathrm{LCP}$, where the polarizations follow the IEEE definition. This is opposite to that historically used by many radio astronomers, who followed the definition of Kraus (1966): $V = \mathrm{LCP} - \mathrm{RCP}$, where the polarizations follow the IEEE definition.
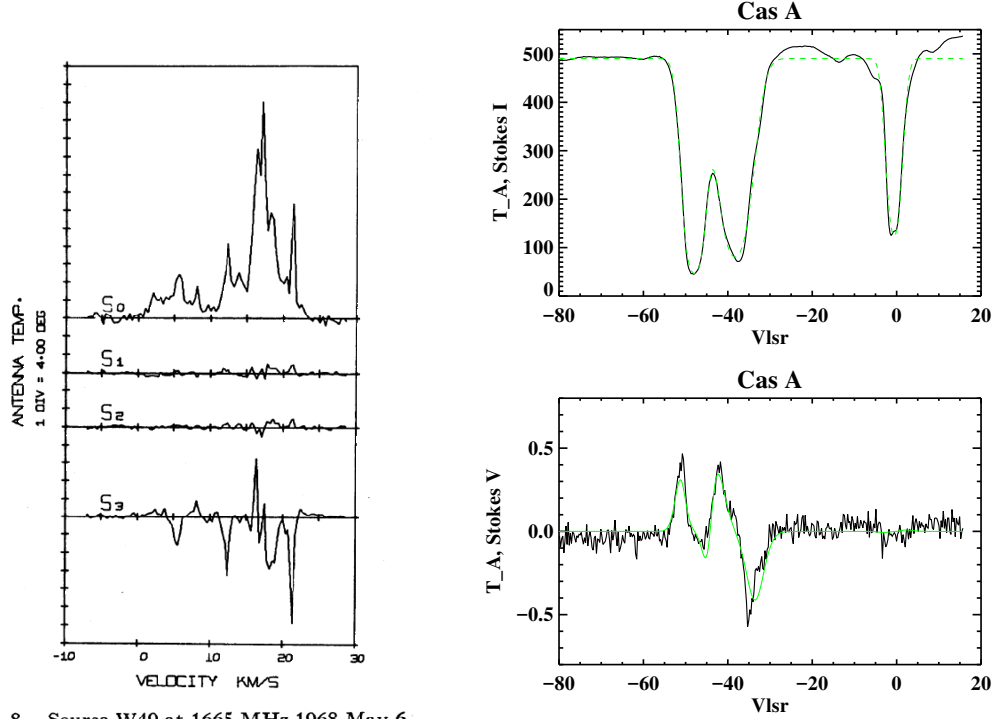
FIG. 8.—Source W49 at 1665 MHz 1968 May 6

Fig. 3.— Left panel: The four Stokes parameters for W49 (Coles & Rumsey 1970). Right panel: Stokes I (top) and V (bottom) for Cas A, from decades-old observations with the Hat Creek 85 foot. In both, Stokes V is plotted according to the IAU convention.

We now always use the IAU-sanctioned definitions: RCP rotates clockwise as viewed by the transmitter, and $V = RCP - LCP$ (IEEE definition).

The 1665 MHz OH maser profile for W49 and the Zeeman splitting of the 21-cm line in absorption against Cas A, shown in Figure 3, are easily detectable and act as a good system and sanity check. Coles & Rumsey (1970), used the IAU definition—even though their work pre-dates the IAU definition!). To our knowledge, the Cas A profile in Figure 3 is the only publicly-available one that follows the IAU definition for Stokes V. Robishaw (2008) stresses that *all* published Stokes V profiles for Cas A either do not follow the IAU convention or are ambiguously or incorrectly defined.

With these definitions, and in addition the common Zeeman convention that *positive B points away from the observer*, the signs of the derived fields are most straightforwardly given by consulting Table 2.2 of Robishaw (2008), which is reproduced here as Figure 4. For emission lines, this figure can be summarized succinctly: *For positive B, RCP lies at a smaller frequency than LCP.*

It is worth more than a footnote to mention here that the convention for magnetic field sign used by radio astronomers making Faraday rotation measurements is exactly opposite to the Zeeman convention. Faraday rotation experts will tell you that a positive field points towards the observer. This convention was arbitrarily chosen by Manchester (1972) because he preferred that a positive rotation measure also correspond to a positive magnetic field (he even points out that this is

TABLE 2.2
MAGNETIC FIELD DIRECTION DETERMINED FROM THE ZEEMAN EFFECT

Field Direction[a]	$\nu_\mathrm{o} - \Delta\nu_\mathrm{z}$	$\nu_\mathrm{o} + \Delta\nu_\mathrm{z}$	Stokes V Profile[b]
Emission Lines			
$B > 0$	RCP	LCP	
$B < 0$	LCP	RCP	
Absorption Lines			
$B > 0$	LCP	RCP	
$B < 0$	RCP	LCP	

[a]A positive magnetic field points away from the observer by convention.
[b]$V = \mathrm{RCP} - \mathrm{LCP}$ by IAU convention (IAU 1974).

Fig. 4.— Obtaining the sign of B from Stokes V, when V is plotted against *frequency*. From Robishaw (2008), Table 2.2.

opposite to the Zeeman convention!). The Zeeman convention has a nice analogue: velocities are also defined to be positive when pointing away from the observer. This convention had been firmly established since the early 1900s, and the early Faraday rotation papers (e.g. Burn 1966) suggest that a positive field also points away from the observer, so it was a questionable decision to have so cavalierly changed the established convention. Clearly for the worse, we are left with this duality in the polarization world and not many astronomers are aware of this. It should be clear that one must be very careful to state one's conventions.

We show two examples of properly-defined Stokes V from real observations. Figure 3 shows the 21-cm line absorption line spectrum for Cas A in Stokes I and Stokes V. The dashed green lines are Gaussian fits with three components. For the three components with velocities $[-48.0, -38.1, -0.7]$ km/s, the derived line-of-sight magnetic field strengths are $[+7.8, +18.1, -0.0]\pm$ $[0.5, 0.6, 0.8]$ μG, respectively. We fitted these components with optical depth profiles using our IDL procedure `tbgfitflex_exp.pro` and we obtained field strengths with `zgfit_selfabs.pro`, both found in `rhstk/procs/zeeman`. Equivalent results can be obtained by fitting negative Gaussians (instead of optical depth profiles) using `gfit.pro` and `zgfit.pro`. These programs give the correct signs of derived fields and return the splitting in units of the horizontal axis, e.g. km/s. One must then convert these velocity-splitting units to Hz and then, for the 21-cm line, divide by the Zeeman splitting coefficient[4] for the 21-cm transition, $b = 2.8$ Hz μG^{-1}. For the software used to obtain this Cas A result, see our illustrative example in §4.4.3.

---

[4]The Zeeman splitting coefficient for a radiative transition depends on the Landé g-factor for that transition and the Bohr magneton; see Heiles et al. (1993) for more details.

3.   ABOUT RHSTK

3.1.   History and Philosophy

Our Robishaw-Heiles SToKes (RHSTK) software, written in IDL, originates from work with the NRAO 140-foot and, particularly, Arecibo in the late 1990's and early 2000's. A few years ago we began to organize this RHSTK restructured version, which is generally applicable and straightforwardly maintainable. 'Generally applicable' means that inputs to procedures are variables and spectra whose format is simple, not tied to any particular telescope, so that the data can be manipulated by standard IDL commands. Thus, this software is applicable at both Arecibo and the GBT—or any other single-dish radio telescope. This document deals with this restructured version.

The RHSTK software contains procedures that accomplish specific calibration tasks. In principle, we could provide 'cookbook' combinations of these procedures that would turn raw data into calibrated data. However, there are many different possible observing modes, which makes it hard to devise cookbooks that cover all possibilities. So we take the alternative approach, in which the observer needs to understand the overall calibration technique and implements it in specific ways for one's own individual observational data set. We attempt to educate the observer on these matters and make things easier by providing examples of commonly-used observational techniques (e.g., frequency switching, position switching), which are given in §4.4.

3.2.   Overview

Fundamentally, there are two basic tasks in all-Stokes calibration. One is to derive the Mueller matrix, which refers to the time-independent portion of the system. The other is to apply the time-dependent calibration and the time-independent Mueller matrix to observational data and derive calibrated all-Stokes spectra. Below, we concentrate on the latter. Deriving Mueller matrices is important, too, but is done much less frequently (because they refer to the time-independent portion of the system); we treat this below in §5 through §6.1.

The calibration process involves the following steps. Each of these is discussed in some detail in sections below.

1. At the GBT, we must produce data files in the format used by RHSTK software (§7.2).

2. Use DIODEON/DIODEOFF data to derive the system gain and phase response (§4.1.1).

3. Use the above-derived system gain and phase response to produce calibrated auto- and cross-product spectra, which we denote by XX, YY, XY, and YX (§4.1.2).

4. Use the above-derived calibrated product spectra to produce Mueller-uncorrected Stokes parameter spectra (§4.1.6).

5. Produce Mueller-corrected Stokes parameter spectra from the above-derived uncorrected ones (§4.1.3).

6. Combine the Mueller-corrected spectra appropriately. This might involve simply data flagging (§4.3) and averaging; alternatively, if you are deriving linear polarization by fitting the parallactic angle variation of Stokes U (§1.6), it might be more involved.

3.3. Overall Observing and Data Reduction Issues

3.3.1. Continuum Observers!!

This memo is written with multichannel spectra in mind. Nevertheless, *even if you are only interested in the continuum*, you must perform the spectral reduction and add up all the spectral points *after* the calibration. You must *not* add them all up beforehand. The reason is the phase change with frequency discussed in §1.3, which is produced by, primarily, the unequal cable lengths between the feed and the spectrometer input. You must correct for this before summing the cross-spectral points.

3.3.2. Spectral Line Observers

For frequency-switched spectra, one often does 'in-band' frequency switching, in which the bandwidth (BW) is about twice the frequency-switching interval and the line appears at different places in the bandpass, usually at about $\frac{BW}{4}$ and $\frac{3BW}{4}$. In this case, you are always observing the spectral line so the concept of the SRCON and SRCOFF spectra doesn't apply. Let's call these two spectra the LO_0 and LO_1 spectra (for the two different LO frequencies). Here, LO_1 is the reference for LO_0 and vice-versa. The proper way to reduce such spectra is to follow the standard procedure for switched spectra *twice*, once using (LO_0, LO_1) for the (SRCON, SRCOFF) spectra and once using (LO_1, LO_0) for the (SRCON, SRCOFF) spectra. With this, you obtain two separate and independent measurements of the line deflection. The line, of course, appears in different spectral channels in these two measurements, separated by the frequency-switching increment. You average these two measurements by shifting the spectra relative to each other.

3.3.3. Mapping

When mapping, you completely sample an area, usually by moving the telescope as you observe with the 'on-the-fly' technique. The best way to process these data is to pick a set of positions in the map that can be regarded as the 'reference', or 'off', positions, and the other positions as 'on' positions. Then you use these as you would use OFFSRC and ONSRC data in treating position-switched data.

3.3.4. Basics and Fundamental Assumptions

For the purposes of description, we implicitly assume native linear polarization. We therefore designate self-products by XX and YY and cross-products by XY and YX, as described in §1.4. After phase and amplitude calibration of the self- and cross-products, the Stokes parameters are given by equation 14. If the system has native circular polarization, then almost everything in this memo remains the same except for some obvious changes, such as (1) X and Y should be replaced by R and L in your mind's eye, and (2) the Stokes parameters are given by equation 15.

We assume you have 'signal' and 'reference' spectra (often called 'SRCON' and 'SRCOFF', or 'SIG' and 'REF'). It's the source *deflection*—the difference between these spectra—that matters. For continuum observations, the SRCON and SRCOFF spectra are nearly always position differences. For spectral line observations, they can be either position differences or frequency dif-

ferences. We also assume that you have calibration data: DIODEON and DIODEOFF spectra. As for the source, it's the Diode *deflection* that matters.

4. CALIBRATING OBSERVATIONAL DATA USING RHSTK AND A KNOWN FEED MUELLER MATRIX $\mathbf{M_{feed}}$

4.1. Using RHSTK to Obtain Calibrated Auto- and Cross-Spectra $[XX, YY, XY, YX]$

We have two levels of these procedures. The lower-level procedures are meant to be flexible enough to use with data from any telescope. The top level properly combines the lower-level procedures and is set up for our observing at the GBT, with data from either the Spectral Processor or the Auto-Correlation Spectrometer. In the examples, and in the discussion below, these top-level procedures are called `init_cal.idl.pro` and `products_to_stokes.pro`. Non-GBT users can look at these two files to see exactly how we invoke the lower-level procedures.

The digital spectrometer produces uncalibrated auto- and cross-spectra, which are subject to the calibration requirements discussed above. There are three essential calibration quantities:

1. A representative value for CpK, which is an average over a portion of the bandpass specified by the spectral channels to include. (This is specified by the vector `gainchnls`; see below.)

2. The linear phase gradient.[5]

3. The bandpass shape. After correcting for the bandpass shape, spectra should be flat unless there are spectral features.

4.1.1. Using the Low-Level Procedures with DIODEON/DIODEOFF Data to Derive the System Gain and Phase Response

To derive the system gain and phase response, we apply the following two procedures to the DIODEON/DIODEOFF data. In the examples (§4.4.1 and §4.4.2) these two procedures are called from the command file `init_cal.idl.pro`, which can be used on any set of GBT data. To obtain the detailed documentation for these procedures, enter IDL and type `doc, 'procedurename'`. The low-level procedures are:

1. The procedure `intensitycal_self, DIODEON, DIODEOFF, gainchnls, tcal, counts_per_k....` This derives the correlator counts per Kelvin from the Diode deflection for a single self-product, e.g. for XX. The inputs are 2d arrays of DIODEON and DIODEOFF spectra, each with dimensions `[nchnls, nspectra]`; and the Diode intensity in Kelvins. A *single* conversion factor `CpK` is calculated from the (mean of DIODEON) − (mean of DIODEOFF) averaged over `gainchnls`. If you want multiple values of `CpK`, e.g. if you want one value for each of the `nspectra` pairs, you need to invoke this procedure once for each on/off pair. This `CpK` factor is used in all subsequent calculations; it is what's usually considered as the 'system gain'.

---

[5]We have not yet implemented the filter phase correction of §1.3, item (4).

You must invoke this separately for XX and YY.

There are two optional outputs, which are usually used only in diagnostics. One is the bandpass shape as given by the average DIODEON spectrum minus the average DIODEOFF spectrum. The other is the Diode-off system temperature averaged over `gainchnls`.

2. The procedure
   `phasecal_cross.pro, diodediffxy, diodediffyx, phasechnls, dpdf, frqbb,`
   `ozero, oslope....` (Here, `frqbb` is the base-band frequency, which is symmetric around 0 Hz. This procedure least-squares fits the relative phase delay between XX and YY to a linear function of frequency, providing the slope (as in equation 1) and the phase at band center. The inputs `diodediffxy, diodediffyx` are the XY and YX Diode deflection spectra, either intensity/bandpass calibrated or uncalibrated[6]; the array of spectral channels to use in the fit (`gainchnls`). The input `dpdf` is the initial guess for the slope (units: radians per MHz); and the array of baseband frequencies corresponding to the deflection spectra (in MHz). The outputs are the fitted slope and zero point for the phase; and the array of phases versus frequency.

   This is a nonlinear fit for $\frac{d\psi}{df}$, so you must enter a reasonably accurate guessed value for the slope (which is `dpdf`). If your guess is too far off the fit will not converge to the correct value, so you need to plot the results and check! To check, use `phaseplot_08, title, frqbb,` `xy, yx, ozero, oslope...`, which has as inputs the baseband frequency array, the XY and YX Diode deflection spectra, and the fitted zero and slope from `phasecal_cross.pro`. This produces a plot that you can look at to evaluate whether the fit gave the right answer.

4.1.2. Applying the System Gain and Phase to the SRCON/SRCOFF Data

The next step is to apply the above-derived system gain and phase response to the ON-SRC/OFFSRC data to produce calibrated auto- and cross-product spectra. In the process, we correct for the bandpass shape. We denote these fully-calibrated self- and cross-product spectra XX, YY, XY, and YX. In the examples (§4.4.1 and §4.4.2) the following low-level procedures are invoked by the high-level procedure `products_to_stokes.pro`, which can be used on any set of GBT data. The low-level procedures are:

1. `self_uncal_to_cal, uncal_on, uncal_off, gainchnls, counts_per_k, cal_on...` This derives `cal_on`, the intensity-calibrated and bandpass-corrected source deflection spectra, by applying the above-determined `CpK` to uncalibrated `uncal_on, uncal_off` (source-on and source-off) data, using `uncal_off` as a reference. The inputs are arrays of uncalibrated SRCON and SRCOFF spectra, with dimensions
   `[nchnls, nONspectra]` and `[nchnls, nOFFspectra]`. It also returns the bandpass shape.

   The SRCONs and SRCOFFs can be paired, or the SRCOFFs can be averaged or medianed. Some people have the erroneous impression that averaging the SRCOFFs produces less noise than using paired SRCONs and SRCOFFs, because then each SRCON is divided by a much less noisy SRCOFF spectrum. However, when you average all the data, this isn't true: the noise in the average is the same (to first order). Generally, using paired SRCONs and SRCOFFs is better, because the SRCOFF spectra might change significantly with time for

---

[6]The intensity calibration doesn't affect relative phase delay.

various and sundry reasons. Hence, we recommend using paired SRCONs and SRCOFFs. You do this by setting the keyword `mean_med_off = 0`.

The calibration that this procedure performs includes (1) converting correlator counts to Kelvins, which is done with `CpK`; and (2) dividing by the bandpass. You must invoke this procedure separately for XX and YY. If you are doing in-band frequency switching, then for each spectral path (like XX) you must invoke this twice, once with (LO_1, LO_0) as the (SRCON, SRCOFF), and again with (LO_0, LO_1) as the (SRCON, SRCOFF); see §3.3.2.

2. `cross_uncal_to_cal, uncal_cross, gainchnls,`
   `xx_counts_per_k, xx_bandpass, yy_counts_per_k, yy_bandpass, cal_cross...` This derives `cal_cross`, the intensity-calibrated and bandpass-corrected spectra for a cross-product, e.g. for XY. The inputs are the array of uncalibrated XY spectra, `gainchnls`, the XX and YY `CpK` (from `intensitycal_self`), and the XX and YY bandpasses (from `self_uncal_to_cal`). The process of calibration includes (1) converting correlator counts to Kelvins, which is done with the geometric mean of the XX and YY values of `CpK`; and (2) dividing by the geometric mean of the XX and YY bandpasses.

   The calibrated cross spectra `cal_cross` are not source-deflection spectra. Rather, they are the corrected version of the input, which is uncorrected. For a given cross-product, e.g. XY, you can run this separately for SRCON and SRCOFF spectra and subtract the calibrated outputs to obtain the calibrated source deflection cross-spectrum; alternatively, you can make SRCON the input uncalibrated spectrum and use an optional input for the uncalibrated SRCOFF spectra.

   You must invoke this separately for XY and YX—and, if you are doing in-band frequency switching, then for each cross-product (like XY) you must invoke this twice, once with (LO_1, LO_0) as the (SRCON, SRCOFF), and again with (LO_0, LO_1) as the (SRCON, SRCOFF); see §3.3.2.

3. `phasecorr_xyyx, xy, yx, frqbb, ozero, oslope, xyc, yxc` This removes the linear phase gradient from the XY and YX spectra. These 'phase-corrected' spectra have zero relative phase delay between the X and Y signal paths, as if the cable length difference $(L_X - L_Y)$ were zero. Inputs are the phase-uncorrected XY and YX spectra, the baseband frequency array, and the derived zero and slope from `phasecal_cross.pro`.

4.1.3. Generating Mueller-Corrected Stokes Vectors from the Mueller-Uncorrected Ones

Next, we use $\mathbf{M_{feed}}$ and $\mathbf{M}_\rho$ to generate $\mathbf{S}_{\rho=0}$ from $\mathbf{S_{obs}}$; and finally, we apply $\mathbf{M_{astron}}$, as in equation 11. $\mathbf{M_{feed}}$ and $\mathbf{M_{astron}}$ are independent of time (i.e., parallactic angle). One must calculate $\mathbf{M}_\rho$ (which depends on parallactic angle) and, then, apply the Mueller matrix (or, rather, its inverse) to the data. This is done with either `mmcorr.pro` or `mm_corr_zmn.pro`.

These two procedures do the same thing, but are invoked in different ways. `mm_corr_zmn`, `m_tot, m_astron, azmidpntn, zamidpntn, stokesc1, npos` inputs the azimuth and zenith angles, calculates the parallactic angles, and does the correction 'in place', meaning that the Mueller-corrected Stokes vectors are returned in the same variable as the original uncorrected ones, thus overwriting the input values. In contrast,
`mmcorr m_tot, m_astron, parallactic_deg, stokesuncal, stokescal` inputs the parallactic angle instead of the azimuth and zenith angles and returns the Mueller-corrected Stokes vectors

as separate arrays, leaving the Mueller-uncorrected vectors alone. In both, there are options for applying only a subset of the Mueller matrices. This is useful, especially, if you want to derive accurate linear polarizations from from native linear feeds and data with a large parallactic angle range (see §1.6).

4.1.4. Fun and Games with `mmcorr`, `mm_corr`, and `mm_corr_zmn`

Since the early days of our all-Stokes software, we have produced four procedures that generate Mueller-corrected Stokes vectors by applying Muller matrix corrections to Mueller-uncalibrated Stokes vectors. These have similar names. In addition, we sometimes use a keyword called `mm_corr`. Accordingly, we offer this note of clarification.

The other two procedures are not used in RHSTK, but were used in an earlier arrangement of our all-Stokes software. They are two versions of `mm_corr.pro` (from 2002-10-26 and 2004-12-29). They were used in spider-scan reductions. To add to the fun and confusion, within RHSTK we sometimes use the parameter `mm_corr` to indicate whether a Mueller matrix correction should be applied to a Stokes vector, but (obviously, we hope) this has absolutely no relation to the earlier `mm_corr.pro` procedures.

4.1.5. The `rcvr` File

Normally one has the Mueller matrix parameters defined in a receiver file, which is generated as discussed in §5.14. These are located in `rhstk/procs/rcvrfiles`. A good example for *native linear* polarization is the standard *L*-band receiver file `rcvr1_2_default.pro`, in which the frequency dependencies of the parameters are defined from multifrequency on/off or spider-scan data. A good example for *native circular* is `rcvr8_10_06jan03.pro`. All receiver files have one input parameter, `cfr`, which is the frequency for which you want the Mueller matrix.

4.1.6. Applying the Mueller Correction with High-Level Software at the GBT

At the GBT, we apply the Mueller corrections (equation 14 or 15) using the high-level procedure `products_to_stokes`.

4.2. Putting it all together

Let's see how the above procedures are used together to form a properly calibrated dataset.

First, deal with the Diode deflections. Suppose we have 10 DIODEON and DIODEOFF spectra, each with 32 channels, in each of two polarizations `xx, yy`; these are the outputs from either a native-linear or native-circular feed. Then we have the self-product arrays `diodeonxx[32,10]`, `diodeoffxx[32,10]` and `diodeonyy[32,10]`, `diodeoffyy[32,10]`; and we have the cross-product arrays `diodeonxy[32,10]`, `diodeoffxy[32,10]` and `diodeonyx[32,10]`, `diodeoffyx[32,10]`. We will use all 32 channels in the calibration. We have Diode values `tcalxx, tcalyy`. We do the following:

```
;DERIVE COUNTS_PER_K FOR XX AND YY...
intensitycal, diodeonxx, diodeoffxx, tcalxx, cts_per_k_xx
intensitycal, diodeonyy, diodeoffyy, tcalyy, cts_per_k_yy

;DERIVE PHASE GRADIENT AND ZERO POINT (ozero, oslope)...
;OUR INITIAL GUESS FOR dp/df IS 0.17 RAD/MHZ...
dpdf = 0.17
;the set of 32 baseband frequencies covers +/- 1.25 MHz
frq= -1.25 + 2.5 * findgen(32)/32.
diodediffxy = diodeonxy-diodeoffxy
diodediffyx = diodeonyx-diodeoffyx
phasechnls = indgen(32)
phasecal_cross, diodediffxy, diodediffyx, phasechnls, dpdf, frq, $
                ozero, oslope

;AFTER DOING THIS FIT, CHECK THE FIT BY LOOKING AT THIS PLOT:
phaseplot_08, 'phase plot example', frq, diodediffxy, diodediffyx, $
        ozero, oslope
```

Next, apply these derived calibration parameters to the data. Suppose we have 60 on-source and off-source self-product arrays in each of two polarizations `srconxx[32,60]`, `srcoffxx[32,60]` and `srconyy[32,60]`, `srcoffyy[32,60]`; and we have the cross-product arrays `srconxy[32,60]`, `srcoffxy[32,60]` and `srconyx[32,60]`, `srcoffyx[32,60]`.

```
;OBTAIN INTENSITY-CALIBRATED SOURCE DEFLECTION SELF-SPECTRA (defln)...
gainchnls = indgen(32)
self_uncal_to_cal, srconxx, srcoffxx, gainchnls, counts_per_k_xx, $
                   deflnxx, bandpassxx
self_uncal_to_cal, srconyy, srcoffyy, gainchnls, counts_per_k_yy, $
                   deflnyy, bandpassyy

;OBTAIN INTENSITY-CALIBRATED ONSRC AND OFFSRC CROSS-SPECTRA (intcal*)...
cross_uncal_to_cal, srconxy, gainchnls,
                    cts_per_k_xx, bandpassxx, cts_per_k_yy, bandpassyy,
                    intcalonxy
cross_uncal_to_cal, srcoffxy, gainchnls,
                    cts_per_k_xx, bandpassxx, cts_per_k_yy, bandpassyy,
                    intcaloffxy
cross_uncal_to_cal, srconyx, gainchnls,
                    cts_per_k_xx, bandpassxx, cts_per_k_yy, bandpassyy,
                    intcalonyx
cross_uncal_to_cal, srcoffyx, gainchnls,
                    cts_per_k_xx, bandpassxx, cts_per_k_yy, bandpassyy,
                    intcaloffyx

;PHASE-CORRECT THE INTENSITY-CALIBRATED CROSS SPECTRA (cal*)...
phasecorr_xyyx, intcalonxy, intcalonyx, frq, ozero, oslope, $
```

```
                 calxyon, calyxon
phasecorr_xyyx, intcaloffxy, intcaloffyx, frq, ozero, oslope, $
                 calxyoff, calyxoff
```

Finally, apply the Mueller matrix corrections to the intensity- and phase-calibrated source deflection spectra. For the self products, e.g. `xx`, the intensity- and phase-calibrated source deflection spectrum is `deflnxx`, which is returned by `self_uncal_to_cal` above; note that `deflnxx` is *not* Mueller-corrected. For the cross products, e.g. `xy`, the intensity- and phase-calibrated source deflection spectrum is `calxyon-calxyoff`; these two quantities come from `phasecorr_xyyx` above. The full Mueller correction includes the parallactic angle correction; below, the array `parangle_deg[60]` contains the parallactic angles in degrees:

```
mm_uncorrdefln = fltarr( 32, 4, 60]
mm_uncorrdefln[ *, 0, *]= deflnxx + deflnyy
mm_uncorrdefln[ *, 1, *]= deflnxx - deflnyy
mm_uncorrdefln[ *, 2, *]= calxyon - calxyoff = deflnxy
mm_uncorrdefln[ *, 3, *]= calyxon - calyxoff = deflnyx
mmcorr, m_tot, m_astron, parangle_deg, mm_uncaldefln, mm_caldefln
```

4.3. Flagging Bad Data

The flagging process for all-Stokes data is best performed by looking at all four Stokes parameters simultaneously, because interference or bad data might show up in only one of the four auto- and cross-product spectra. We constructed a procedure that displays a set of all four Stokes spectra as four grayscale images. This makes it easy to examine all four simultaneously. It is always our philosophy that even if only one of the Stokes parameters is suspect, all four should be discarded.

This program is called `flag_rfi.pro`. It is best run with a large screen monitor because the grayscale images are displayed side-by-side.[7] It can be employed at any stage in the process: uncalibrated auto- and cross-product spectra, calibrated ones, Mueller-uncorrected Stokes spectra, Mueller-corrected Stokes spectra. We provide an example in §4.4.1.

4.4. Illustrative Examples of Reducing Frequency- and Position-Switched Data

The RHSTK subdirectory contains documentation, procedures, and examples. The examples are provided for three reasons: (1) to ensure that you have properly configured GBTIDL; (2) to provide real data so you can familiarize yourself with how things work and how calibrated results should look; and (3) to provide a sample command file for reducing data on which your own requirements can be set.

---

[7] We had a difficult time making `flag_rfi.pro` work on a MacBook Pro running OS X Lion. First, we need to tell OS X to allow IDL windows to get focus when clicked, so at a command line, type `defaults write com.apple.x11 wm_click_through -bool true` (this only needs to be done once ever). Then, if using Xquartz X11, go to Preferences and select "Emulate three button mouse" in the Input tab; in the Windows tab, select "Click-through Inactive Windows". These latter steps allow you to hold Option while clicking to emulate a middle mouse click, or Command while clicking to emulate a right mouse click. If using some other X11, there should be similar options in the Preferences for that version of X11.

We provide two types of examples for reducing data, frequency switched (`fswitch`) and position switched (`pswitch`).[8] Accessing the examples is simple if you have created the symbolic link to the `rhstk` directory under the `gbtidlpro` directory in your home directory as we described in §7.1: from the Linux prompt in your home directory, type `cd gbtidlpro/rhstk/rhstk_examples`, list the contents, and `cd` to the chosen example's subdirectory. Then look at the README file, which tells how to invoke the associated command files and run-time files; it also provides some commentary. A command file with name `command.idl.pro` is initiated by typing `@command.idl`; a run-time file with name `runtime.idlprc.pro` is initiated by typing `.run runtime.idlprc`.

4.4.1. Frequency Switching

This example resides in `rhstk/rhstk_examples/fswitch/bgdata` and is an example of 'in-band' frequency switching (see §3.3.2). The datafile contains two structures: `src`, which stores the on-source data and contains 98 elements, and `cal`, which stores the calibration data and contains 9 elements (you can see this by typing `help, src, cal`). The `cal` data are interspersed with the `src` data. The datastream begins with a Cal measurement, which has `cal.scannum=6` and consists of two spectra, one with Diode on and one with Diode off. Every 12th scannum is a Diode measurement: thus, `src.scannum=[7-17, 19-29, ...]` and `cal.scannum=[6,18,30,...]`. Thus, the observing consists of groups of 12 scan numbers, the first of which is a Diode measurement and the next 11 are source measurements.

The `src` data are frequency switched. Each subscan contains two spectra, one at each frequency. Each scan contains 8 subscans (the number of subscans are stored in `src.nsubscan`). Thus each scan contains 16 spectra, arranged in 8 subscans with each subscan having a single pair of the two frequencies. Each `cal` measurement has a single subscan, which contains both the DIODEON and DIODEOFF measurements.

The output is calibrated Stokes spectra, which are on-freq − off-freq. For in-band frequency switching, there are two sets of Stokes spectra, as discussed in §4.1. We store the Mueller-corrected frequency-switched Stokes spectra in `src_fsw_cal`, whose tags are identical to the original `src` structure. Thus the output consists of 98 switched, calibrated sets of 16 spectra apiece. The 16 spectra within each scan derived from 8 pairs of LO_0 and LO_1 `src` spectra.

These are 21-cm line data. As discussed in §1.7, 21-cm line Stokes V spectra are contaminated by the responses from polarized sidelobes. This example contains a calculation of these responses.

4.4.2. Position Switching

This example resides in `rhstk/rhstk_examples/pswitch/artiedata`. The datafile contains two structures, `src` (58 elements) and `cal` (15 elements). The `src` data are position switched, with alternate scan numbers being on and off source. Thus, `src[0]` is on source, `src[1]` is off source, etc. The `cal` data are interspersed with the `src` data. The datastream begins with a Cal measurement, which consists of two spectra, one with Diode on and one with Diode off; this has `cal.scannum=1`. Every fifth scannum is a Cal measurement: thus, `src.scannum=[2,3,4,5,7,8,9,10,12,13,14,15,...]` and `cal.scannum=[1,6,11,...]`. Thus, the observing consists of groups of five scan numbers, the first of

---

[8] We also provide two types of examples for determining Mueller matrices; see §5 and §6.

which is a Cal measurement and the next four are source measurements. Each `cal` measurement has a single subscan, which contains both the DIODEON and DIODEOFF measurements. Each `src` measurement has 237 subscans, all of which have identical observing parameters (such as being on source or off source).

You can distinguish between on source and off source scans by the `src.subscan.cra2000`, which is the right ascension in hours; on-source measurements are at higher right ascension. The idea of this position-switched measurement was to cover the same hour-angle range for the on-source and off-source measurements within each pair. Each source scan lasts 4 minutes of time, so the on- and off-source right ascensions are separated by one degree. Within each on/off pair, the on-source data were taken first, so covering the same hour angle range within each pair would require the off-source right ascension to be higher than the on-source one; the opposite occurred, which was a mistake in setting up the observing file.

The calibrated Stokes parameters refer to the source deflection. Thus there are half as many calibrated spectra as there are on- and off-source uncalibrated spectra. We write the calibrated position-switched spectra into the structure `src_psw_cal`, whose tags are identical to those in the on-source counterpart of the uncalibrated `src` structure. Thus the output of this Stokes calibration calculation consists of 29 switched, calibrated sets of 237 spectra apiece. These are derived from 29 pairs of on- and off-source `src` spectra.

4.4.3. Determining Zeeman Splitting Using RHSTK Software

Two examples reside in `rhstk/rhstk_examples/zeeman`. One, in the subdirectory `hatcreek`, contains (1) a model profile generated numerically, and (2) high S/N data on Cas A from observations using the old Hat Creek 85-ft. The other, in the subdirectory `gbt`, contains recent low S/N data on Cas A from the GBT. The examples illustrate how to fit Gaussians to emission and absorption line data and how to derive independent field strengths for the individual components.

5. DERIVING THE TOTAL SYSTEM MUELLER MATRIX (new, heavily revised section as of 25jun2017)

5.1. The importance of, and the definition of, the parallactic angle

To evaluate the Mueller matrix parameters, we fit the observed pseudo-Stokes parameters to their variations with parallactic angle ρ. The parallactic angle ρ is important because it is the position angle at which the feed samples the source. As such, it interchanges polarized power between Stokes Q and U according to the Mueller matrix

$$\mathbf{M_{SKY}} = \begin{bmatrix} 1 & 0 & 0 & 0 \\ 0 & \cos 2\rho & \sin 2\rho & 0 \\ 0 & -\sin 2\rho & \cos 2\rho & 0 \\ 0 & 0 & 0 & 1 \end{bmatrix}. \tag{16}$$

The central 2×2 submatrix is, of course, nothing but a rotation matrix.

Question: just exactly what do we mean by this parallactic angle ρ? It is conceptually easier to think in terms of native linear polarization, so we discuss this case first and designate *AMB* by the more descriptive $XX - YY$, etc, where XX is the X self-product, etc.

5.1.1. A Native dual-linear feed

The parallactic angle of importance is that of the feed probe that we are calling X. This is easy to see: The observed Stokes parameter $Q_{obs} = XX - YY$. For a source whose polarization position angle $\theta_{src} = 0°$ (i.e., its polarization is north-south with no east-west component), Q_{obs} is maximized when the X probe is north-south, i.e. when the X probe's parallactic angle is zero.

The relationship between the source's parallactic angle and the X probe's parallactic angle depends on how the feed is mechanically mounted on the telescope. Consider the telescope being pointed towards zenith. In this case, the parallactic angle equals the azimuth angle + 180 degrees. For polarization, this 180 degrees might as well be zero degrees because polarization is concerned with orientation, not direction, so for now we will forget about the 180 degrees and consider the two angles to be equal. Place yourself at the feed looking down at the ground. You see azimuth increase clockwise; parallactic angle also increases clockwise. If the X probe is aligned north-south, then both its azimuth and its parallactic angle are zero. If the X probe is rotated clockwise by some angle θ_{feed}, then both its azimuth and its parallactic angle equal θ_{feed}.

Now consider the telescope being pointed towards some source. Define a new spherical coordinate system whose pole is the direction of the source; call this the z axis. The two linear probes are two orthogonal lines that define a plane. This plane is perpendicular to the line of sight to the source, so we can call this the x-y axes of the new coordinate system. In this new system, the relationship among the telescope, feed, and sky are identical in spirit to the telescope pointing towards the zenith in the terrestrial alt-az system, with the exception that for $\theta_{feed} = 0$ the parallactic angle of the X-probe ρ_X is equal to the parallactic angle of the source, ρ_{src}. So, generally, we can write

$$\rho_X = \rho_{src} + \theta_{feed} \qquad (17)$$

In our least squares fits for the parallactic angle dependence of the observed Stokes parameters, we should be using ρ_X as the independent variable.

5.1.2. A Native dual-circular feed

For native circular polarization the concept of θ_{feed} remains valid. For native circular, ψ defines the position angle of linear polarization of the feed; knowing ψ, one could make a mark on the feed itself to indicate the equivalent orientation of the X probe. Having done that, the discussion for a dual-linear feed applies for dual-circular, too.

In principle, one could measure ψ in the lab and thereby derive the equivalent θ_{feed} for the circular feed. In practice, we want to do this astronomically to have confidence. Moreover, the equivalent θ_{feed} would be a linear function of frequency unless cable lengths for the two polarizations were equal.

5.2. Source Selection and Parallactic Angle Coverage

Classically, one derives the Mueller matrix from a series of scans on a polarization calibration source such as 3C286. This series should cover a substantial range in parallactic angle; the larger the range, the more accurate the result. So request telescope time and plan your observations accordingly! The polarization memo by Heiles and Fisher (1999) contains a list of suitable polar-

ization calibrators at 1.4, 5, 8, and 14 GHz. You can use our IDL routine `find_gbt_polcal` to plot the parallactic angle swing of the Heiles & Fisher calibrators as a function of LST (read the documentation for details). Figure 5 shows the parallactic angle swing for a set of calibrators over the LST range 8–16 hours.
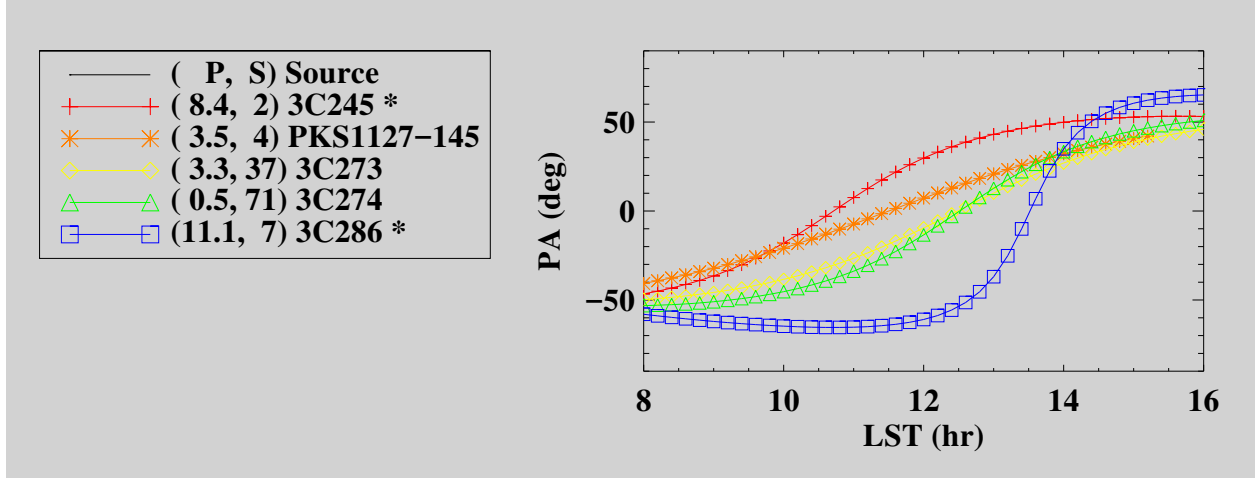

Fig. 5.— Parallactic angle swing for some polarization calibrators over the LST range 8–16 hours. The legend lists the calibrators along with their total flux density S in mJy and the percentage polarization P at 4.8 GHz. This plot was made by `find_gbt_polcal`.

5.3. The Mueller Matrix and its Parameters

We least-squares fit the self- and cross-products to parallactic angle ρ. If the feed Mueller calibration were already perfect, then both the total intensity, Stokes I, and the circular polarization, Stokes V would be independent of ρ; and the two linear-polarization Stokes parameters, Q and U, would vary sinusoidally with 2ρ. The departure from these ideals defines the Mueller matrix of the feed.

The primary and most important output of our Mueller-matrix calibration software is a plot showing the four calibrated correlator products versus parallactic angle. It also lists the values of the derived parameters and prints the associated Mueller matrix. The plot is useful to assess the quality of the fit and to obtain human-readable Mueller matrix parameter values. Figure 6 shows an example.

The Mueller matrix has 16 elements, but there are only 7 independent parameters. In fact, for our formulation, one of these parameters (χ) is constrained to equal $\pi/2$, and another (`angle_astron`) specifies the telescope's zero of position angle of linear polarization and is transferred to the "astronomical" Mueller matrix $\mathbf{M_{astron}}$, so there are only 5 independent parameters. These are described in detail by Heiles et al. (2001b). Of these, three are the most important because they describe zeroth-order effects, while four are less important because they describe imperfections such as nonorthogonality in the polarizations, so for high-quality feeds (like most of the GBT feeds!) they are very small. The parameters, listed in order of their typical importance in real life, are:

1. $\mathbf{\Delta G}$ is the error in relative intensity calibration of the two polarization channels. It results from an error in the relative cal values (T_{calA}, T_{calB}). Our expansion currently takes terms in ΔG to first order only, so if the relative cal intensities are significantly incorrect then the

other parameters will be affected. The relative cal values should be modified to make $\Delta G = 0$, keeping their sum the same. To accomplish this, make $T_{calA,modified} = T_{calA}\left(1 - \frac{\Delta G}{2}\right)$ and $T_{calB,modified} = T_{calB}\left(1 + \frac{\Delta G}{2}\right)$.

Having $\Delta G \neq 0$ is not a serious problem as long as it is not *too* different from zero. Our treatment of the Mueller matrix coefficients assumes that off-diagonal Mueller matrix elements are small, i.e., we include them only to first order. So if $\Delta G = 0.1$, you incur an error of 0.01 because of our first-order treatment. You can either live with the $\Delta G \neq 0$, or you can change the assumed Diode temperatures to achieve the condition $\Delta G = 0$.

2. ψ is the phase difference between the cal and the incoming radiation from the sky. It redistributes power between (U, V) for a dual linear feed and between (Q, U) for a dual circular feed. polarizations. We have two cases:

   (a) Native linear polarization. If the cables connecting the correlated Diode to the feed are of identical length and the r.f. paths through the feed are identical for the two polarizations (the thick lines in Figure 1), then $\psi = 0$. If the cable lengths differ, then $\psi \neq 0$. Moreover, in this case we expect $\psi \propto \nu$, where ν is the r.f. frequency. Therefore, if you are making measurements at different frequencies, you should include this frequency dependence in the specification for ψ. See the example rcvrfile `rhstk/procs/gbtprocs/rcvrfiles/rcvr1_2__default.pro`.

   (b) Native circular polarization. In this case, the phase difference ψ determines the angle of linear polarization for Stokes Q and U. This is indeterminant from our least-squares fit for $\mathbf{M_{feed}}$. Accordingly, for native circular we force $\psi = 0$ and don't fit for it; we use $\mathbf{M_{astron}}$ to empirically obtain the correct position angle of linear polarization. **IS THIS WHAT WE REALLY DO? SHOULD RETHINK!!!** Because ψ depends linearly on frequency, so too will this correction to the position angle for native circular. This correction is specified by the parameter called `angle_astron`, which depends linearly on frequency unless the cable/propagation lengths are equal for the two polarizations. This is unlikely in practice! See the example native-circular rcvrfile `rhstk/procs/gbtprocs/rcvrfiles/rcvr8_10__06jan03.pro`.

3. α is a measure of the voltage ratio of the polarization ellipse produced when the feed observes pure linear polarization. Generally, the electric vector traces an ellipse with time; $\tan \alpha$ is the ratio of major and minor axes of the voltage ellipse. Thus, $\tan^2 \alpha$ is the ratio of the powers. If a source having fractional linear polarization $P_{src} = \sqrt{Q_{src}^2 + U_{src}^2}$ is observed with a native circular feed that has $\alpha = \frac{\pi}{4} + \delta\alpha$, with $\delta\alpha \ll 1$, then the measured Stokes V will change sinusoidally with 2ρ and have peak-to-peak amplitude $4\delta\alpha$. α might also be a function of frequency, particularly for native circular. See the example native-circular rcvrfile `rhstk/procs/gbtprocs/rcvrfiles/rcvr8_10__06jan03.pro`.

4. χ is the relative phase of the two voltages specified by α. Our analysis assumes $\chi = 90°$; this incurs no loss of generality.

5. ϵ is a measure of imperfection of the feed in producing nonorthogonal polarizations (false correlations in the two correlated outputs). Our expansion takes ϵ to first order only. The only astronomical effect of nonzero ϵ is to contaminate the polarized Stokes parameters (Q, U, V) by coupling Stokes I into them at level $\sim 2\epsilon$; the exact coupling depends on the other parameters. For weakly polarized sources, this produces false polarization; for strongly polarized sources such as pulsars, it also produces incorrect Stokes I.

6. ϕ is the phase angle at which the voltage coupling ϵ occurs. It works with ϵ to couple I with (Q, U, V).

7. $\boldsymbol{\theta_{astron}}$ is the angle by which the derived position angles must be rotated to conform with the conventional astronomical definition.

The observing system consists of several distinct elements, each with its own Mueller matrix. The matrix for the whole system, $\mathbf{M_{TOT}}$, is the product of the individual Mueller matrices. Each Mueller matrix element is a combination of one or more of the system parameters summarized above. In calculating $\mathbf{M_{TOT}}$, we set $\chi = 90°$. We ignore second order terms in the imperfection amplitudes $(\epsilon, \Delta G)$ but, of course, retain all orders in their their phases (ϕ, ψ) and also in the feed parameter α. This gives

$$\mathbf{M_{TOT}} = \begin{bmatrix} 1 & (-2\epsilon\sin\phi\sin 2\alpha + \frac{\Delta G}{2}\cos 2\alpha) & 2\epsilon\cos\phi & (2\epsilon\sin\phi\cos 2\alpha + \frac{\Delta G}{2}\sin 2\alpha) \\ \frac{\Delta G}{2} & \cos 2\alpha & 0 & \sin 2\alpha \\ 2\epsilon\cos(\phi+\psi) & \sin 2\alpha\sin\psi & \cos\psi & -\cos 2\alpha\sin\psi \\ 2\epsilon\sin(\phi+\psi) & -\sin 2\alpha\cos\psi & \sin\psi & \cos 2\alpha\cos\psi \end{bmatrix} . \quad (18)$$

The terms in the top row make $I \neq 1$ for a polarized source. If one derives fractional polarization, for example $\frac{Q}{I}$, then it will be in error by amounts comparable to $[(\epsilon, \Delta G) \times (Q, U, V)]$. For the frequent case of a weakly polarized source, these products are second order and therefore are of no concern. However, for a strongly polarized source such as a pulsar or OH maser, these terms are first order.

5.4. The digital backend outputs

If our digital backend is a correlator (the XF technique), then our measured quantities are four time averaged voltage products from the digital correlator: from autocorrelation, $(E_A E_A, E_B E_B)$; from crosscorrelation, $(E_A E_B, E_B E_A)$. In these products we consider the second quantity to be delayed relative to the first. Each correlation function has N channels of delay. We Fourier transform (FT) these quantities to obtain spectra. The autocorrelation functions are symmetric and thus their FT's are real, with no imaginary components. We combine the two measured crosscorrelation functions into a single one with $2N$ channels; it has both negative and positive delays and is generally not symmetric, so its FT is complex. If our digital backend is a FFT device (the FX technique), then the above operations are performed in the backend and the outputs are the same. See Robishaw & Heiles (2017) for details.

For both XF and FX, we phase and amplitude calibrate the power spectra outputs using a correlated noise source and then combine these calibrated spectra a pseudo-Stokes vector:

$$\mathbf{S_{pseudo}} = \begin{bmatrix} APB \\ AMB \\ AB \\ BA \end{bmatrix} = \begin{bmatrix} FT(E_A E_A) + FT(E_B E_B) \\ FT(E_A E_A) - FT(E_B E_B) \\ 2\operatorname{Re}[FT(E_A E_B)] \\ 2\operatorname{Im}[FT(E_A E_B)] \end{bmatrix} . \quad (19)$$

If we have an ideal native dual linear feed and a perfect receiver, then $\mathbf{S_{pseudo}} = (I, Q, U, V)$; for native circular, $\mathbf{S_{pseudo}} = (I, V, U, -Q)$.

5.5. Least-Squares Fitting for the Mueller Matrix Parameters

Classically, we evaluate the parameters in equation 18 using observations of a polarized calibration source tracked over a wide range of parallactic angle ρ. The source is described by $\mathbf{S_{src}}$ and the Mueller matrix for the radiation entering the feed by $\mathbf{M_{sky}}$. The full Mueller matrix is $\mathbf{M_{TOT}} \cdot \mathbf{M_{sky}}$. The product of this matrix with $\mathbf{S_{src}}$ results in a set of of four equations, one for each element of the observed $\mathbf{S_{pseudo}}$ vector. Expressed in terms of matrices, these equations are

$$
\begin{bmatrix} APB \\ AMB \\ AB \\ BA \end{bmatrix} = \mathbf{M_{TOT}} \cdot \mathbf{M_{SKY}} \cdot \begin{bmatrix} I_{src} \\ Q_{src} \\ U_{src} \\ V_{src} \end{bmatrix} . \tag{20}
$$

In practice, we cannot reliably measure the ρ dependence of APB because it is rendered inaccurate by small gain errors. Thus, in practice we use fractional correlator outputs and fractional source polarization. We define

$$
\mathbf{S'_{pseudo}} = \frac{\mathbf{S_{pseudo}}}{APB} \tag{21}
$$

and

$$
\mathbf{S'_{src}} = \frac{\mathbf{S_{src}}}{I_{src}} \tag{22}
$$

and consider only the last three equations in equation 20. We also take $APB = I_{src}$ instead of $APB \approx I_{src}$. This gives

$$
\begin{bmatrix} 1 \\ AMB' \\ AB' \\ BA' \end{bmatrix} = \mathbf{M_{TOT}} \cdot \mathbf{M_{SKY}} \cdot \begin{bmatrix} 1 \\ Q'_{src} \\ U'_{src} \\ V'_{src} \end{bmatrix} . \tag{23}
$$

Note that the division by APB produces errors in the elements of $\mathbf{S'_{pseudo}}$, but these errors are second order because they are products of ΔG and/or ϵ with quantities such as Q_{src} that are already first order. Our whole treatment neglects second order products, so we can neglect these errors.

Suppose there are N measurements of $\mathbf{S_{pseudo}}$. These could be a single source at N parallactic angles, N different sources each at one parallactic angle, or some combination, with some sources measured at more than one parallactic angle. For each observation, equation 23 gives the relation between the observed fractional pseudo-Stokes vector, the known parallactic angle, and the calibration source's known fractional Stokes vector. The product $\mathbf{M_{TOT}} \cdot \mathbf{M_{SKY}}$ involves the 5 Mueller matrix parameters in equation 18 and the parallactic angle. Given a set of N observations, deriving the Mueller matrix parameters involves using a nonlinear least-squares fit of the observed pseudo-Stokes parameters to the source Stokes parameters, which is a somewhat cumbersome process.

There are two ways to perform this least-squares fit. One is for the general case in which one observes a set of different calibration sources, each with its own *different* set of parallactic angles. The other is for the case of one or more calibration sources, all of which have the *same* set of parallactic angles. For a single source, such as the gold-standard calibrator 3C286, this is the classical case. Closely related is the case of multiple sources, *all* having the *same* set of parallactic angles; in real life, this is useful for the case of polarized masers.

5.6. The General Case, `mparamsfit.pro`: N observations of different polarization standard calibrators

We have N equations like equation 23. We write out the matrix elements explicitly; the matrix product is

$$\mathbf{M_{TOT}} \cdot \mathbf{M_{SKY}} = \begin{bmatrix} m_{II} & m_{IQ} & m_{IU} & m_{IV} \\ m_{QI} & m_{QQ} & m_{QU} & m_{QV} \\ m_{UI} & m_{UQ} & m_{UU} & m_{UV} \\ m_{VI} & m_{VQ} & m_{VU} & m_{VV} \end{bmatrix} . \tag{24}$$

The matrix elements are just the partial derivatives, for example

$$m_{VQ} = \left. \frac{\partial AMB'}{\partial Q_{src'}} \right|_{U_{src}, V_{src}} . \tag{25}$$

Each matrix element such as m_{VQ} is a complicated function of the 5 Mueller matrix parameters $(\alpha, \epsilon, \phi, \Delta G, \psi)$; these functions are given by comparing equation 24 with equation 18. We use the usual nonlinear least squares fitting procedures to solve for them, and use numerical techniques to obtain the relevant derivatives.

5.7. The Classical Case, `mmfit_2016.pro`: A single polarization calibration source (e.g. 3C286) observed at N parallactic angles

This is the 'classical case' because it is the simplest and most direct way to obtain the Mueller matrix coefficients. As a bonus, it can also, if desired, provide the Stokes parameters of the source. This is a two-step process.

The first step is fitting the parallactic angle behavior of each of the 3 observed pseudo-Stokes parameters:

$$AMB' = A_{AMB'} + B_{AMB'} \cos 2\rho + C_{AMB'} \sin 2\rho . \tag{26}$$

Figure 6 shows fits for an example. With three coefficients for each of the three pseudo-Stokes parameters we have a total of 9 coefficients. The coefficients (A, B, C) are complicated functions of the 5 parameters $(\alpha, \epsilon, \phi, \Delta G, \psi)$ and, also, the three source Stokes parameters $(Q_{src}, U_{src}, V_{src})$. To determine these functions, we regroup equation 20 in terms of the sinusoidal behavior of the three pseudo-Stokes parameters:

$$\begin{bmatrix} AMB' \\ AB' \\ BA' \end{bmatrix} = \begin{bmatrix} (m_{II} + Vm_{IV}) & (Qm_{IQ} + Um_{IU}) & (-Qm_{IU} + Um_{IQ}) \\ (m_{QI} + Vm_{QV}) & (Qm_{QQ} + Um_{QU}) & (-Qm_{QU} + Um_{QQ}) \\ (m_{UI} + Vm_{UV}) & (Qm_{UQ} + Um_{UU}) & (-Qm_{UU} + Um_{UQ}) \\ (m_{VI} + Vm_{VV}) & (Qm_{VQ} + Um_{VU}) & (-Qm_{VU} + Um_{VQ}) \end{bmatrix} \cdot \begin{bmatrix} 1 \\ \cos(2\rho) \\ \sin(2\rho) \end{bmatrix} . \tag{27}$$

The second step uses the 9 coefficients from the first step as the input data for a nonlinear least squares fit to determine the 5 Mueller matrix coefficients and, if desired, the 3 pseudo-Stokes parameters of the source.
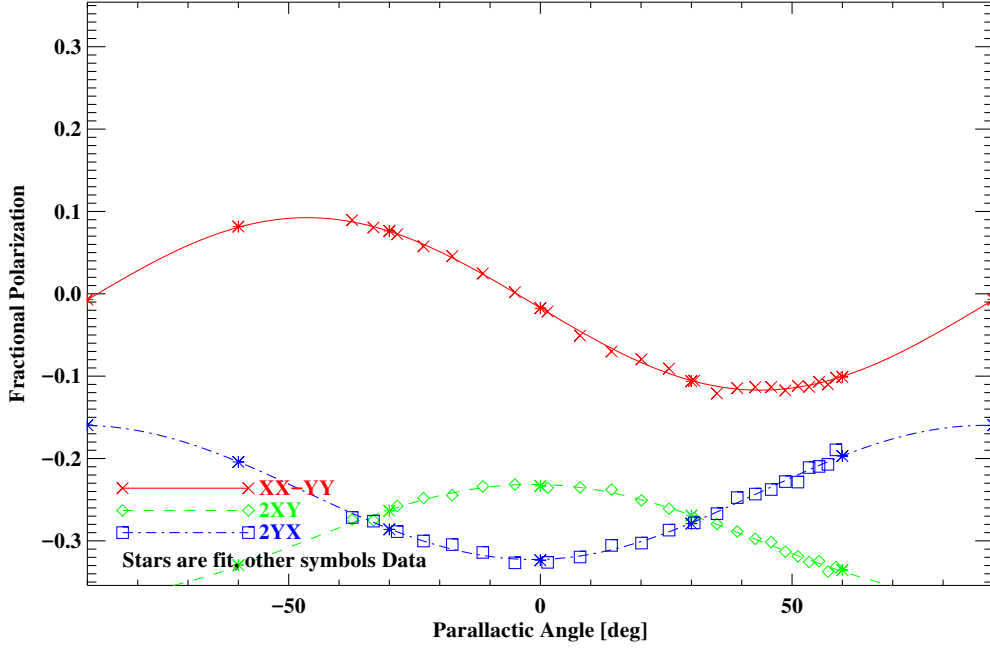
SRC = W49_3867
DELTAG = −0.025 ± 0.002
PSI = +128.9 ± 0.2
ALPHA = +0.0 ± 0.0
EPSILON = +0.000 ± 0.000
PHI = +0.0 ± 0.0
CHI = +90.0 ± 0.0
Q_{SRC} = −0.005 ± 0.001
U_{SRC} = −0.105 ± 0.001
U_{SRC} = +0.385 ± 0.001
POL_{SRC} = +0.106 ± 0.001
PA_{SRC} (**UNCORRECTED FOR M_{ASTRO}**) = −46.43 ± 0.23
──

Mueller Matrix:

```
    1.0000   −0.0123    0.0000    0.0000
   −0.0123    1.0000    0.0000    0.0000
    0.0000    0.0000   −0.6279   −0.7783
    0.0000    0.0000    0.7783   −0.6279
```

Fig. 6.— Fitting results for channel 3867 of W49 with the successful guess $\alpha = 0$.

5.8. The Expanded Classical Case, `mmfit_2016_multiplesources.pro`: Multiple polarized sources (e.g. W49 Maser), all observed at the same set of N parallactic angles

This is just like the Classical Case, except that there can be more than one source. This was written to derive Stokes parameters for multiple line components in an OH maser.

5.9. Commentary on some fundamentals

Nonlinear least squares fitting is often plagued by multiple minima, and the present case is no exception. Heiles et al. (2001b) discuss these in some detail; here we only summarize some of the degeneracies.

1. For native linear polarization, one cannot distinguish between the two cases $(\alpha, \psi) = (0°, \psi_0)$ and $(\alpha, \psi) = (90°, \psi_0 + 180°)$. For these two cases, the signs of (Q, U) change, which is equivalent to rotating the feed by 90°. For a conventional linear feed, loosely described as two E-field probes in a circular waveguide, the combination $(\alpha, \psi) = (90°, 180°)$ is physically unreasonable.

2. For native circular polarization, the position angle of the source $2PA_{src}$ and ψ are inextricably connected. We can determine only their sum (for $\alpha = 45°$) or their difference. In particular, the two solutions $\alpha = 45°$, $\alpha = -45°$ are degenerate; the two solutions have different signs for Q_{src}, thereby rotating the derived PA_{src} by 90°).

   The physical interpretation of this degeneracy is straightforward: for a pure circular feed, the phase of a linearly polarized source rotates with 2ρ and its absolute value depends both on the system phase ψ and the source position angle PA_{src}. There is no substitute for an independent calibration of the linearly polarized position angle, either with a test radiator or with a source of known polarization.

3. ϵ is the quadrature sum of the ρ-independent portions of the two correlated outputs (AB, BA). This power is distributed between those outputs according to $(\phi + \psi)$. In the near-linear case, ψ can change by 180° by changing the choice for α, and this also produces a 180° change in ϕ.

4. Consider a high-quality standard linearly polarized feed that has a correlated cal connected by equal-length cables. Such a feed has $\alpha \approx 0°$ and the equal-length cables mean that $\psi \approx 0°$. However, the solution yields $\psi \approx 180°$ if the sign of AMB is incorrect, which can easily happen if one interchanges cables carrying the two polarizations; this is equivalent to reversing the handedness of ρ and PA_{src}.

5. We have adopted the following procure for phase calibration. If there is a correlated cal then we measure ψ_{cal} and fit it to a constant plus a slope $\frac{d\psi}{df}$; we subtract this fit from the source phase and produce corrected versions of (AB, BA). Thus, the only component left in the correlated products is the difference between source and cal phase, which is the same as ψ.

6. The position angle of the source polarization PA_{src} is defined relative to the local idiosyncrasies. Astronomers need to follow the IAU conventions for parameter definitions; for polarization, the most important are the definition of position angle and the sign Stokes V. These matters are discussed in detail by Robishaw & Heiles (2016). To satisfy this requirement, we may need to apply a rotation matrix $\mathbf{M_{astron}}$, which looks like $\mathbf{M_{SKY}}$ in equation 16 with ρ replaced by θ_{astron}, and in the bottom diagonal element has the possibility of reversing he sign of V. Finally, at low frequencies, one must include the effects of terrestrial ionospheric Faraday rotation, which is time variable.

5.10. Comparison of our three Mueller matrix parameter fitting programs

Given observed polarized sources, we have the abovementioned three programs that fit the data to provide the Mueller matrix elements:

5.10.1. mmfit_2016.pro

Given a single polarized source observed over a range of parallactic angles, this least squares fits the data to provide the Mueller matrix parameters. This is our classic fitting procedure, modified to allow nonzero Stokes V. It is intended for the very common case where you have well-sampled parallactic angle covereage of a single polarization calibration standard source.

The input data consist of the ρ dependences of each of the 3 observed fractional Stokes parameters, which are expressed by 3 parameters for each observed Stokes parameter. For example, for AMB we have

$$AMB = A + B\cos(2\ PA_{az}) + C\sin(2\ PA_{az}) \tag{28}$$

The coefficients (A, B, C) are fitted to the observed fractional Stokes parameters by stripfit_to_pacoeffs. Thus, there are 9 input numbers (3 sets of (A, B, C), one for each of the three fractional Stokes parameters).

These 9 coefficients then serve as the inputs to the nonlinear fit for the Mueller matrix parameters and source Stokes parameters. There are up to 8 parameters to fit: 5 Mueller matrix parameters and 3 source Stokes parameters (Q', U', V'). You can choose any combination of the 8 parameters to fit. For example, if you know the source Stokes parameters, you specify that they not be fit. Because the number of fitting parameters can be as high as 8, and there are only 9 inputs, the more parameters you can fix, the better. When you fit for all 8 parameters, there is only 1 degree of freedom, and the degeneracies (covariances) might be strong and the fit can become unstable. It is probably best that you do not include all 8 parameters in the fit. In our classic fits, we forced the Stokes V parameter to equal zero, because our calibration sources were classic continuum sources with very little V; this worked well. Now, however, we might want to use OH masers, which can have strong Stokes V.

The nonlinear least squares fit requires initial guesses for the parameters to be solved for. It is OK to set the initial guesses for the source Stokes parameters to zero. However, if you set the initial guesses for 5 the Mueller matrix parameters to zero and fit for all 8 parameters, the fit will not properly converge. The initial guesses for the 5 matrix parameters need to depart a bit from zero; our default is 0.001. These are generated by the program mm_coeffs_in_setup.pro. Alternatively, you can exclude one or more parameters from the fit, setting its value by hand equal to a constant.

With nonzero V, you should eliminate other parameters from the fit. The most important Muellar matrix parameters are ΔG and ψ, and you always need to solve for them. Because a reasonably well-engineered feed will have small imperfections, the parameters that express these imperfections can be eliminated from the fit. These parameters are ϵ and its associated phase angle ϕ; and α and its associated angle χ. Almost always, ϵ is the least important parameter because it is the smallest. For any native polarization you can set $\epsilon = 0$ and its angle to anything and not solve for them. This should be enough to obtain a good fit. You can reduce covariance problems further by fixing α: for native dual linear you set $\alpha = 0°$ and $\chi = 90°$; for dual circular, $\alpha = 45°$ and $\chi = 90°$. The program never allows a fit for χ, which should always be set to 90°.

5.10.2. mmfit_2016_multiplesources.pro

This is like mmfit_2016.pro, but treats the case when you have observations of more than one source and want to derive Mueller matrix parameters by including the data from all those sources.

You can also obtain the Stokes parameters for all, or any combination of, the sources.

The most important use for this is when you have well-sampled ρ coverage of a polarized OH maser, e.g. W49, for which you can regard each spectral channel as an independent source. The program then provides not only the Mueller matrix parameters, but also the 3 Stokes parameter spectra. For each source (or spectral channel), the input data consist of the ρ dependence of each of the 3 observed fractional Stokes parameters, which is expressed by 3 parameters for each observed Stokes parameter—a total of 9 data points for each source. The total number of input datapoints is then $9N_{src}$.

If you don't know the source polarizations, then you are fitting for 5 Mueller matrix elements plus 3 Stokes parameters per source. The total number of fitting parameters is $5 + 3N_{src}$. So the number of degrees of freedom is the difference between these two numbers, which is $6N_{src} - 5$. So having only just two sources instead of one has a big effect because it changes the number of degrees of freedom from 1 to 7. Nevertheless, if the feed is good you still might want to not fit for ϵ and ϕ, and maybe also α. We have little experience for real-life data, so explore.

A caution for large N_{src} (e.g., hundreds or thousands of channels in a single spectrum): The number of parameters being solved for is $5 + 3N_{src}$. Suppose $N_{src} = 1000$, i.e. you have a three 1000-channel spectra (one for each fractional Stokes parameter)—so $3N_{src} = 3000$. The covariance matrix is then a 3005 x 3005 matrix, and the program has to evaluate its inverse. The computer time required for matrix inversion goes as $(3N_{src} + 5)^3$. !!CUBED!! When N_{src} exceeds a few hundred, the time can become excessive. You can deal with this in a two-step fashion: step 1, rebin the spectra so that you have fewer channels, and do the fit at lower spectral resolution; step 2, apply the derived mueller matrix to the spectra with full resolution.

The comments §5.10.1 above apply here equally well.

5.10.3. mparamsfit.pro

This program determines Mueller matrix parameters when you have observations of 2 or more sources and little or no parallactic angle coverage. You have to know the polarizations of the observed sources. For example, if you have observations of several continuum polarization standard calibrators, each at 1 or more parallactic angles, this will provide the Mueller matrix parameters. But it cannot provide the source Stokes parameters; you have to know them and provide them as inputs.

The FAST and Galt telescopes need this program because of their limited or zero coverage in parallactic angle. The sources can be continuum polarization calibrators or a known OH maser spectrum; the latter is especially convenient because you don't have to do position switching.

For each observed source, the input data are its 3 observed fractional polarized Stokes parameters, so the number of input datapoints is $3N_{src}$. There are five Mueller matrix parameters to solve for, so with 2 sources there is 1 degree of freedom (but see paragraphs below). As in §5.10.1, this might not be enough, so you might need to exclude ϵ and ϕ, and maybe also α, from the fit. The more sources, the better; the fewer parameters to solve for, the better.

5.11.   The Subleties of the Nonlinear Fit for the Mueller Matrix Parameters

This fit uses the 9 outputs of rhe first fit as inputs to derive the Mueller matrix parameters. Thus, the input is the set of 9 independent datapoints. The full suite of unknowns comprises 8: 5 Mueller matrix parameters (ΔG, ψ, α, ϵ, ϕ); and 3 source parameters (Q_{src}, U_{src}, V_{src}). If you solve for all 8 parameters, there is only one degree of freedom! This can make the solution unstable because of covariances. If you think the feed is good, with no crosscoupling between the feed outputs, then exclude ϵ and ϕ from the fit. And, expecially for native linear feeds, exclude α also; setting it to zero is usually an excellent approximation. For native circular, however, you may need to include α (using a guessed value of $\pi/4$) because native circular feeds often have a substantial response to linear polarization—whicih is often significantly frequency-dependent.
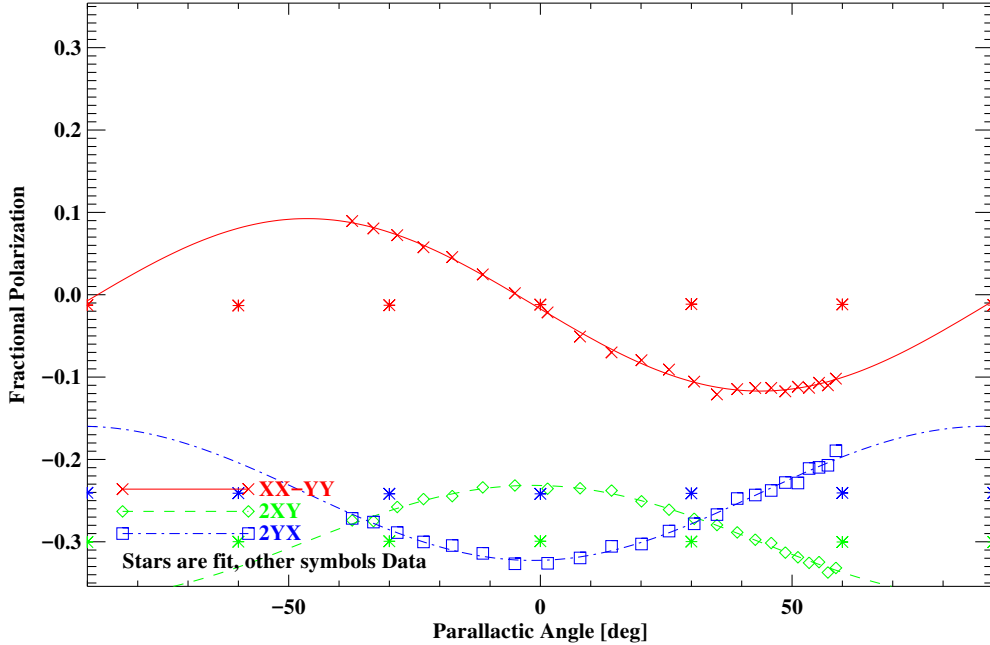
SRC = W49_3867
DELTAG = −0.025 ± 0.149
PSI = −51.2 ± 11.1
ALPHA = +0.0 ± 0.0
EPSILON = +0.000 ± 0.000
PHI = +0.0 ± 0.0
CHI = +90.0 ± 0.0
Q_{SRC} = +0.000 ± 0.053
U_{SRC} = +0.001 ± 0.053
U_{SRC} = −0.385 ± 0.075
POL_{SRC} = +0.001 ± 0.053
PA_{SRC} (**UNCORRECTED FOR M_{ASTRO}**) = +34.08 ± ******
−−

Mueller Matrix:

1.0000	−0.0123	0.0000	0.0000
−0.0123	1.0000	0.0000	0.0000
0.0000	0.0000	0.6268	0.7792
0.0000	0.0000	−0.7792	0.6268

Fig. 7.— Fitting results for channel 3867 of W49 with the unsuccessful guess $\alpha = 0$.

Figures 6 and 7 show the fitting results for an elliptically-polarized OH maser component in W49, for two different guesses for α. On each figure, the AMB curve (in red, with crosses) is labelled XX-YY; the AB curve (in green, with diamonds) is labelled 2XY; and the BA curve (in blue, with squares) is labelled 2YX. These curves and their points are the fit (1) above, using

`stripfit_to_pacoeffs.pro`. The astericks, which are not connected by lines, are the nonlinear fit (2) above.

Figure 6 is a successful fit because the astericks lie on their associated curves. In contrast, Figure 7 shows an unsuccessful fit because the astericks don't. In fact, this is one of those cases where the fit converged not to a *minimum* of the sum-of-squares $\Sigma\sigma^2$ of the residuals, but a *maximum!* This can happen because the least-squares fit technique finds solutions for which the first derivative of $\Sigma\sigma^2$ with respect to the parameters is zero—whether or not this represents a minimum or a maximum.

The former fit is successful because the guessed value of α was close enough; the latter, not. By experimenting, we found that obtaining a successful fit required the guess for α to be within $\pm 1.06 \times \pi/2$ radians of its correct value (which is 2.25 radians). Whether or not this range for success is general is unknown. The message: *in all nonlinear fits, look at the results* and if they are unsatisfactory, try different input guesses!

Finally: after deriving the Mueller matrix, you need to check a *second* linearly-polarized calibration source by observing, calibrating, and Mueller-correcting it. This observation can be quick—just a single on/off will do. The reason is to make sure that the 'handedness' of the position angle of linear polarization is defined properly, i.e., that position angle increases from North towards the East. This has to do with the ambiguity in sign for Stokes Q in equation 15 in §1.5.3. For example, at 1420 MHz the gold-standard polarization calibration source 3C286 has a position angle of about 28° and 3C454.3 has 70°; the difference is +42°. If one used only 3C286 and adjusted **M$_{\text{astron}}$** accordingly, and if the handedness were incorrect, then 3C454.3 would be measured as $28° - 42° = -14°$ instead of $28° + 42° = 70°$.

5.12.   The New Software and an Example

As of Aug2016, this nonlinear fit is done with `mmfit_2016.pro`; in previous times we used `mm_genfit.pro`. The main improvements are (1) we now include the possibility of a nonzero Stokes V for the source being fit, which is necessary when using OH masers and pulsars for Mueller matrix calibration, and (2) we allow you to exclude any combination of parameters from the fit, which is handy for high-quality feeds and sparse measurements.

The new software resides in
`/dzd4/heiles/rhstk/procs/mueller_2016`
An example of `mmfit_2016` using observational data for this software resides in
`/rhstk/rhstk_examples/mueller_2016/from_dec2016`
An example using fake data for all three programs in §5.10 resides in
`/rhstk/rhstk_examples/mueller_2016/from_dec2016`.

5.13.   The Old Software and Examples

For the old software, We provide two examples:

1. One example, using the same GBT data as in the position-switching example above in §4.4.2, resides in `rhstk/rhstk_examples/mueller/artiedata`. The file `gbt_artie_tst.idlprc.pro` uses `mm_genfit.pro` and the file `gbt_artie_idlprc.pro` uses `mmlsfit.pro`.

2. The other example uses Arecibo position-switched data, which were calibrated with our Arecibo polarization-reduction software and uses GBTIDL to derive the feed Mueller matrix. This example resides in `rhstk/rhstk_examples/mueller/aodata`. It uses `mmlsfit.pro`.

5.14. Frequency Dependence of Mueller Matrix Coefficients and the `rcvr` File

If you are observing spectra centered at a single frequency, you don't usually need to worry about frequency dependencies of the derived Mueller-matrix coefficients. However, this is not always the case; for example, if you use the L-band receiver to observe both OH at 1667 MHz and HI at 1420 MHz, you need to worry about the frequency dependence.

You need to have a file that contains the relevant information. In RHSTK, we call these "rcvr-files". They are generated by hand using the parameters derived by our Mueller-matrix calibration software. An example for L-band is `rhstk/procs/gbtprocs/rcvrfiles/rcvr1_2_default.pro`. This file specifies the 7 Mueller matrix coefficients (see below) and their frequency dependencies. The Mueller matrix itself is calculated from these coefficients using the procedure `rhstk/procs/mueller/m_tot.pro`.

6. DERIVING MUELLER MATRICES FROM SPIDER SCANS

6.0.1. What is a Spider Scan?
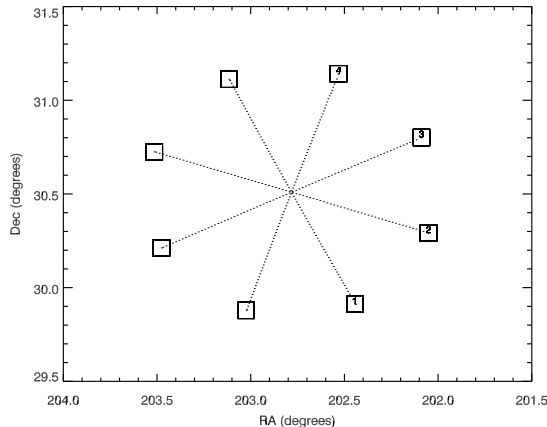
Fig. 8.— A spider scan. Two of the four scans are oriented along $\Delta AZ, \Delta ZA$; the other two are oriented at 45° to these. As a result, their orientation in $(\Delta RA, \Delta \delta)$ space depends on the hour angle.

Spider scans consist of four scans across the source separated by angles of 45°, as shown in Figure 8. The advantage of using spider scans is that they allow determination of not only the on-axis Mueller matrix, but also the structure of the telescope beam in all four Stokes parameters (see §6.1). Until the recent past, this was the only way our software could obtain the feed Mueller matrix. We provide two examples of spider-scan reductions, one for native linear and one for native circular, in `rhstk/rhstk_examples/spider`.

6.0.2. Reducing Spider Scan Data

The default settings for plotting and printing produce the output described below. These settings are specified in `cal01.idl.pro`, which has appropriate, if somewhat cryptic, documentation. You can change any of these parameters except ones having to do with actual calculations. With the settings used in the example files (`spider_tst_linear.idl.pro` and `spider_tst_circular.idl.pro`), these programs produce the following output:

1. A plot on the lower right, in IDL plot window 1, of the i.f. phase versus baseband frequency in MHz. Data are in white, the linear fit of phase to frequency is in red. The fit should be excellent. If it's not, there's a reason: this is a nonlinear least-squares fit, so it requires a guess for the phase gradient, and if the guess is too far off, the nonlinear fit won't converge properly.

    The upper right plot in IDL window 0 contains the phase versus frequency for the source deflection. If the source is unpolarized, the phase cannot be reliably determined, so the plot is meaningless in this case. If the source is linearly polarized, then the phase changes with parallactic angle. There is no useful information in this plot except to show that the source is polarized; perhaps the main function of this plot is to amuse the person running the software.

2. For each spider scan, it prints the derived phase slope in the command window. This slope should be essentially identical for all scans.

3. For each spider scan, in window 31 it plots the four correlator outputs versus position along the four spider arms. Meanwhile, windows 0 and 1 are displaying grayscale images of the first sidelobe and the main beam.

4. In the command window, it prints the derived beam parameters for each spider scan.[9] When it says something about Stokes parameters (e.g. Stokes V) it's a lie, because you haven't done the polarization calibration yet; instead of Stokes parameters, these are the uncalibrated correlator products. You obtain the true Stokes beam parameters below in §6.1.

5. At the very end, it plots the correlator outputs versus parallactic angle, together with the least-squares fit; from this fit, it derives the Mueller matrix parameters, which are given on this plot (as seen in Figure 9).

6. When you've done the calibration, it is good to check it by Mueller-correcting the original input data and making sure that, with those Mueller-corrected data, the derived Mueller coefficients are zero to within the uncertainties. The example file `spider_tst_linear.idl` shows how to do this. Figure 10 shows the Mueller-corrected data from Figure 9.

If the parameters `saveit` and `ps1yes` are set, then for the series of spider scans two sets of files are produced, each with a `.sav` and a `.ps` file. (These parameters are *not* set in the example files to prevent permission problems in writing these output files.) One set of files is prefixed with `mm4` and the other with `mm4_2d`. The former contains results derived by treating each of the scans through the source as an independent entity; thus, for each spider scan, there are four independent scans. The latter contains results derived by treating each spider scan (which consists of the set of four individual scans) as an independent entity. Thus, the `mm4` plots contain 4 times as many points

---

[9]Quantities like aperture efficiency rely on proper source fluxes and Diode values, so may not be correct. See §6.1.

Rcvr1_2 1666 MHz BRD0 5.0 MHz SP 3C286 14–JUL–2010

DELTAG = −0.014 ± 0.008
PSI = −20.8 ± 2.5
ALPHA = +0.7 ± 1.2
EPSILON = +0.005 ± 0.002
PHI = +7.9 ± 22.3
Q_{SRC} = −0.043 ± 0.003
U_{SRC} = −0.086 ± 0.003
POL_{SRC} = +0.096 ± 0.003
PA_{SRC} (**UNCORRECTED FOR M_{ASTRO}**) = −58.15 ± 0.88
NR GOOD POINTS: X−Y = 12   XY = 12   YX = 12 / 12
––
Mueller Matrix:

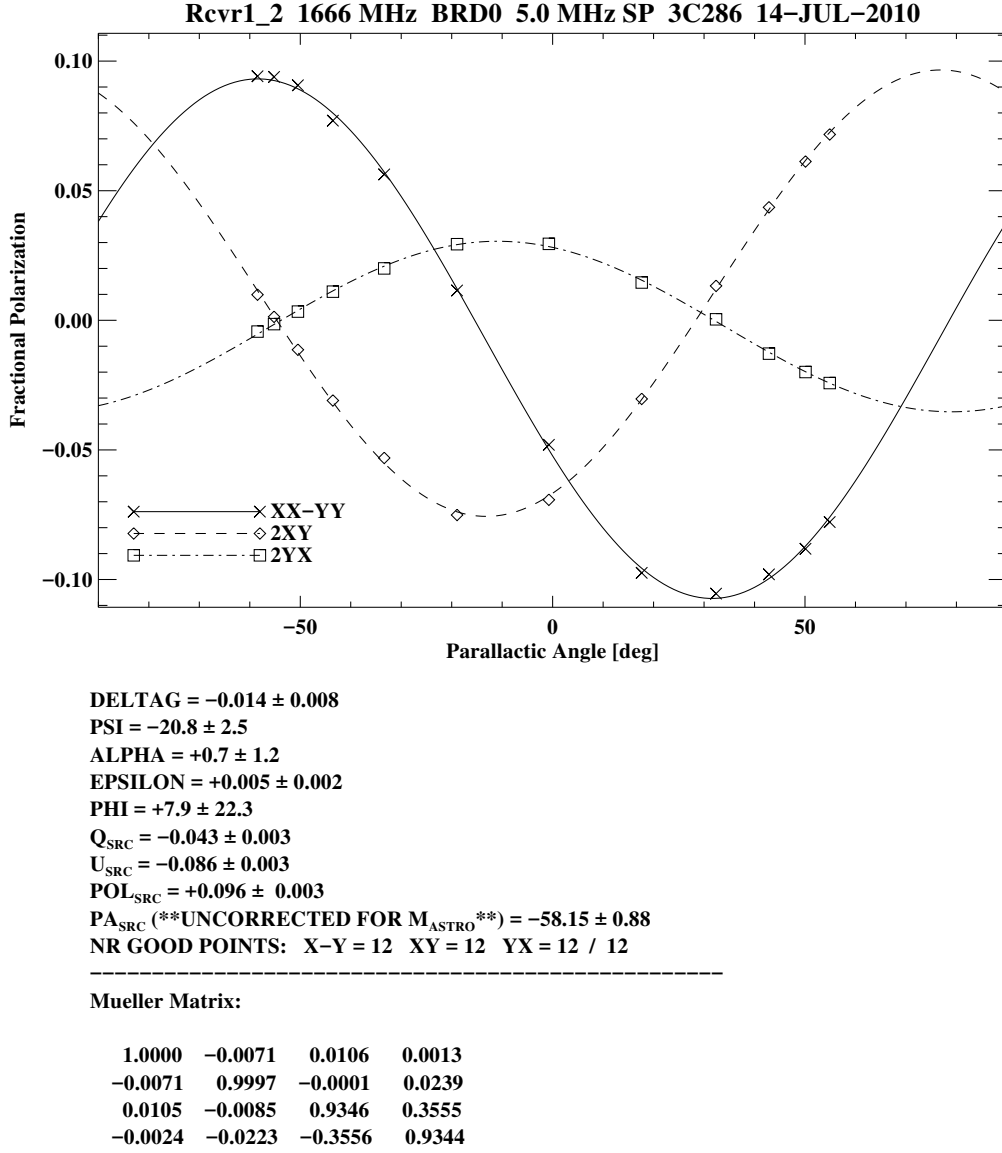|			
1.0000	−0.0071	0.0106	0.0013
−0.0071	0.9997	−0.0001	0.0239
0.0105	−0.0085	0.9346	0.3555
−0.0024	−0.0223	−0.3556	0.9344

Fig. 9.— Example of the PostScript output from the RHSTK Mueller calibration software.

as do the mm4_2d plots. The mm4_2d plots are better, in principle, because the effects of pointing errors are accounted for. However, if the source is changing parallactic angle rapidly, the set of four scans that constitute a spider scan smear over a range of parallactic angle. Usually the results are imperceptibly different. Use your judgement to decide which results to accept. The two sets of files are:

1. A PostScript (PS) file, which duplicates the above-mentioned plot of the four correlator products versus parallactic angle and, also, lists the values of the derived parameters and the Mueller matrix. The plot is useful to assess the quality of the fit and to obtain human-readable Mueller matrix parameter values. Figure 9 shows an example of an mm4_2d plot.

2. An IDL save file, with a .sav extension, which contains data that are used in subsequent polarization calibration of data. This save file contains:

   (a) The structure muellerparams1, which contains derived Mueller parameters and other info.

Rcvr1_2 1666 MHz BRD0 5.0 MHz SP 3C286 14–JUL–2010
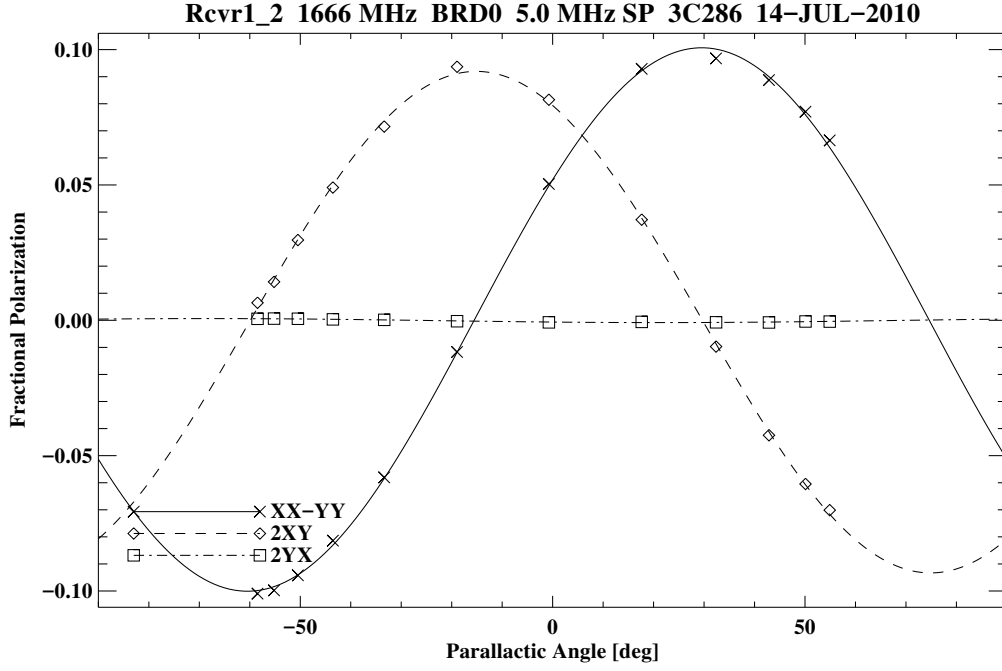
DELTAG = 0.001 ± 0.008
PSI = −0.1 ± 2.3
ALPHA = +0.2 ± 1.2
EPSILON = +0.000 ± 0.002
PHI = −171.4 ± 328.6
Q_{SRC} = +0.049 ± 0.003
U_{SRC} = +0.083 ± 0.003
POL_{SRC} = +0.097 ± 0.003
PA_{SRC} (**UNCORRECTED FOR M_{ASTRO}**) = +29.70 ± 0.82
NR GOOD POINTS: X−Y = 12   XY = 12   YX = 12 / 12
––
Mueller Matrix:

1.0000	0.0003	−0.0007	−0.0001
0.0003	1.0000	−0.0000	0.0071
−0.0007	−0.0000	1.0000	0.0022
−0.0001	−0.0071	−0.0022	1.0000

Fig. 10.— Example of the PostScript output from the RHSTK Mueller calibration software showing the data in Figure 9 after Mueller correction.

(b) The structure `a`, which stores various astronomical info such as parallactic angle, source info. . .

(c) The structure `beamout_arr`, which contains info about the beam pattern (beamwidth, etc.). The tag `beamout_arr.b2dfit` is a 50-element array that contains the derived beam parameters; for definitions, see `rhstk/procs/spider/beam2dfit.pro`.

(d) The structure `muellerparams_chnls`, which contains info on a channel-by-channel basis. This is usually not used because calculating it is time consuming. If you want to do this, you can do this by setting `chnl=1` in the file `cal01.idl.pro` (or, setting it after `cal01.idl` is invoked).

6.1. Deriving Polarized Beam Parameters from Spider Scans

Spider scans also provide the beam properties in all Stokes parameters (point-source gain, beamwidth, beam ellipticity, coma, squint, squash, and the first-sidelobe structure). These parameters are described by Heiles et al. (2001); also, see our GBT Commissioning Memo 23 (Heiles et al. 2003), which shows beam-calibration results for L-band, C-band, and X-band.

The derived parameters include aperture and beam efficiency, for which it needs source fluxes and also accurate Diode temperatures. Source fluxes are in the file `rhstk/procs/calib/fluxsrc.dat`.[10] You must use the correct source name for the software to find your source flux. If it cannot find the source flux, it assigns a flux of -1 Jy (that's minus one Jy). If your source isn't in there, you can add it; stick to the format in that file. If your source is time-variable, or if you have a more accurate flux than exists in this file, you can change it.

The spider scan software produces beam maps for the given input data, which are Mueller uncorrected. Thus, the beam maps are not maps for true Stokes parameters, unless you specify that the input data are to be corrected. To accomplish this, you must specify that the input data be Mueller corrected, which you do by setting the Mueller correction parameters, and providing a feed Mueller matrix to correct with by specifying the `rcvr` file name. These are shown in the example file `spider_tst_linear.idl`. The derived beam parameters reside in the structure `beamout_arr.b2dfit` ; see §6.

7. USING RHSTK AT THE GBT

7.1. Incorporating RHSTK into GBTIDL

Incorporating RHSTK software into GBTIDL is simple. The RHSTK subdirectory simply needs to be placed into the set of subdirectories scanned by GBTIDL. The easiest way to do this is to place a symbolic link to the subdirectory that contains the RHSTK procedures under the `gbtidlpro` subdirectory in your home directory. If you are running on the Green Bank computers, you do this by making a symbolic link: from the linux prompt, type

```
> ln -s /users/cheiles/rhstk $HOME/gbtidlpro
```

Alternatively, you can put the RHSTK subdirectory on the set of paths scanned by GBTIDL. To do this, after entering GBTIDL type the IDL command

```
GBTIDL> addpath, '/users/cheiles/rhstk/procs', /expand
```

Finally, if you are running GBTIDL on your own computer, then copy /users/cheiles/rhstk to a suitable place on your own filesystem and refer to that.

7.2. Producing Files with the RHSTK Format

At the present time (Summer 2013), GBT polarization observations can be done either with the Green Bank Spectrometer or the Spectral Processor. In the near future, both will probably

---

[10]We thank Chris Salter and Phil Perillat at Arecibo for providing this file. Formatwise, it's not very pretty, but if you want to read it yourself badly enough, you can figure it out!

replaced by the VErsatile Gbt Astronomical Spectrometer (VEGAS). There may be some glitches when the current RHSTK software is applied to VEGAS data.

RHSTK uses IDL structures as variable types instead of the 'container' type format used by GBTIDL. Producing GBT data in the proper format for RHSTK is a two step process: **(1)** 'filling' the data with `sdfits`; and (2) converting the data to RHSTK format with `sdfits_to_rhstk`.

7.2.1. 'Filling' GBT Data with `sdfits`

GBT observational data reside in many different files. Some contain telescope data such as pointing positions, some contain environmental data, some contain the spectrometer output. The necessary relevant data must be gathered and written into a single file, a process known as 'filling'.

Filling is accomplished by the GBT procedure `sdfits`, which is run on GB computers as a standalone program. It produces files known as 'SDFITS files', which are FITS files with names like `AGBT09C_065_03.raw.acs.fits`. Here, the `AGBT09C_065` is the project ID and the `03` is the session number in GBT parlance (e.g., the 3rd observation period for this project ID). The `raw` means the data are uncalibrated, which is the default option when running `sdfits`; for polarization, we must calibrate the data ourselves! The `acs` means the Auto-Correlation Spectrometer (the alternative is `sp`, for Spectral Processor). The `.fits` suffix means this is a standard FITS file. You run the program `sdfits` from the Linux prompt; see the GBTIDL manual for details.

`sdfits` is run automatically as you take your GBT data. So, in principle, you don't need to run it again. However, for organizational purposes you might wish to run it again, running it for particular sets of scan numbers to create a separate output file for each. For example, you might wish to produce `fits` files that contain only one source in each session, instead of all sources in each session.

For our purposes, running `sdfits` is simple because all of the options are properly set by default. You need to know the project ID; you need to know which spectrometer you used; and you need to know the scan numbers to process. A real-life example was

```
> sdfits -backends=acs -scans=1:75,77:86,90:109 AGBT09C_065_02
```

This writes the FITS file into the disk area from which you run the program; alternatively, you can specify the output disk area.

Normally, of course, you'd like to include and process all of the scans. However, often there are problems during the datataking. In particular, `sdfits_to_rhstk` requires that every scan has all of the expected subscans, so if an observation was manually interrupted in the middle of a set of subscans, then that entire scan number must be discarded. To determine the scan/subscan content, run our program `scancheck`[11] from the GBTIDL prompt:

```
GBTIDL -> scancheck, 'AGBT09C_065_02'
```

It produces a 3-column list. The first column is the scan number, the second is the number of subscans, and the third is the source name. Exclude anything that looks irregular. If in doubt,

---

[11]If `scancheck` crashes it will almost certainly be because the directory structure has been changed by the GBT software engineers. If so, the file `getgbtdatapath.pro` needs to be changed accordingly. The data archive directory structure is located in `/home/archive` on the Green Bank system.

include data; and if `sdfits_to_rhstk` crashes, exclude them.

7.2.2. A Caution About Using `sdfits` on pre-2006 Data

GBT data that were taken before sometime in 2006 need to be treated cautiously. Such data are saved with FITS version of 1.3 (in the header, it shows up as `FITSVER=1.3`) . When you convert raw data to SDFITS format using the `sdfits` command on a GBT machine, everything runs fine no matter what `FITSVER` the data are saved in. However, you will not be able to convert the `sdfits`-converted data to an `RHSTK` IDL structure if the data were taken before early 2006. The current quick fix is to convert the raw data by using the `sdfits-test` command instead of `sdfits`.

7.2.3. Converting SDFITS to RHSTK Format Using `sdfits_to_rhstk`

The next step is to convert to the simple RHSTK format. You do this within GBTIDL using our procedure `sdfits_to_rhstk.pro`. Looking at its documentation, you'll find three input parameters:

1. `FILESIN` — a list of input SDFITS files, including the path. It runs through them sequentially and produces an IDL save file for each, with names that are automatically generated. An example:
   `bgpos11_acs_Rcvr1_2_12.5_1_09Dec30_21:43:56.sav`
   `bgpos11` is the source name, `acs` means it used the spectrometer, `Rcvr1_2` means the *L*-band receiver, `12.5` means the observed bandwidth was 12.5 MHz, the `_1_` tells which correlator section (IF number for the spectrometer), and finally the date and time.

2. `PATHOUT` — the path to the subdirectory where to write the output save files.

3. `BINDOWN=BINDOWN` — Tells how many spectral channels you want in the spectra that are written to the IDL save file. For the spectrometer, there can be up to 16384 channels per spectrum, which is usually more than you want and provides too much resolution (and gigantic data files!). Set `BINDOWN` to the number of channels that you would like to be saved. `BINDOWN` must be a power of 2, e.g. 512. The Spectral Processor, in contrast, will never produce spectra with more than 1024 spectral channels, so there's no strong need to bin down these spectra.

Frequency-switched and position-switched data are treated in the same fashion. For these cases, the `sdfits_to_rhstk.pro` output save files contain two arrays of structures, `src` and `cal`[12]. The tags of each structure contains all timing, angle, status, and other information, and are appropriately named. The structures also contain the structure `subscan`, which has each spectrum within the scan plus all ancillary information such as Diode state, position, etc.[13] The `src` structures contain on/off source data and the `Diode` structures contain on/off Diode data. There is an explicit assumption that a Diode scan not only has the `Diodestate` flag set, but also that there is only *one* subscan. **We do not employ a winking Diode, the GBT default, but instead fire the high Diode on then off for a brief period before an on-source scan begins, leaving**

---

[12]In IDL you can see the contents (called 'tags') of a structure (e.g., named `src`) by typing `help, src, /st`

[13]In GBT parlance, our subscan is known as an integration.

the Diode off during all on-source scans. This results in a scan that contains one subscan with a Diode-on phase and a Diode-off phase. If your Diode scans have more than a single subscan then you must modify the software to suit your observing set-up.

The other type of observation supported by `sdfits_to_rhstk.pro` is the "spider scan". This is a standard observing mode on the GBT (see §6). The output save files for spider scans contain three arrays of structures, `CalBefore`, `Strip`, and `CalAfter`. They are processed by the RHSTK package to determine Mueller matrices and beam properties.

8.   OBSERVING POLARIZATION AT ARECIBO

We have used Arecibo extensively for spectrolarimetry. We support only one kind of observation: frequency- or position-switched observations using the interim correlator. We routinely use a command file that controls the telescope and datataking without human intervention. Ask one of the accomplished Arecibo observers about how to observe; these include Carl Heiles, Tim Robishaw, and Allison Smith, among others.

Having obtained the data, you use our reduction procedures as described in `heiles/tim_a2119/test_school/stg0.notes`. This produces data that are fully Stokes calibrated. However, it does not perform the bandpass correction. This final step is done by `arecibo_uncal_to_cal.pro`, which is located in `rhstk/arecibo`

REFERENCES

Bode, H. W. 1940, "Relations Between Attenuation and Phase in Feedback Amplifier Design", Bell Sys. Tech. J., 19, 421

Boothroyd, A. I., Blagrave, K., Lockman, F. J., Martin, P. G., Pinheiro Gonalves, D., & Srikanth, S. 2011, "Accurate galactic 21-cm H I measurements with the NRAO Green Bank Telescope", A&A, 536, 81

Burn, B. J. 1966, "On the depolarization of discrete radio sources by Faraday dispersion", MNRAS, 133, 67

Coles, W. A., & Rumsey, V. H. 1970, "Stokes Parameters for OH Sources", ApJ, 159, 247

Heiles, C., & Fisher, R. 1999, "Calibrating the GBT for Spectral Polarimetry Using Cross Correlation", NRAO electronics Division Internal Reports 309. Unfortunately, this is not available on NRAO's web page. For an electronic copy, see http://astro.berkeley.edu/~heiles/handouts/handouts_radio.html

Heiles, C., Goodman, A. A., McKee, C. F., & Zweibel, E. G. 1993, in Protostars and Planets III, ed. E. H. Levy & J. I. Lunine (Tucson: Univ. Arizona Press), 279

Heiles, C., Perillat, P., Nolan, M., Lorimer, D., Bhat, R., Ghosh, T., Howell, E., Lewis, M., O'Neil, K., Salter, C., & Stanimirović, S. 2001a, "All-Stokes Parameterization of the Main Beam

and First Sidelobe for the Arecibo Radio Telescope", PASP, 113, 1247

Heiles, C., Perillat, P., Nolan, M., Lorimer, D., Bhat, R., Ghosh, T., Lewis, M., O'Neil, K., Salter, C., & Stanimirović, S. 2001b, "Mueller Matrix Parameters for Radio Telescopes and Their Observational Determination", PASP, 113, 1274

Heiles, C., Robishaw, T., Troland, T., & Roshi, A. 2003, "Calibrating the GBT at L, C, and X Bands", available at
http://www.gb.nrao.edu/~rmaddale/GBT/Commissioning/index.html

IAU 1974, in Transactions of the IAU, Vol. XVB 1973, Proceedings of the Fifteenth General Assembly, ed. G. Contopoulos & A. Jappel (Dordrecht: Reidel), 165

Kraus, J. D. 1966, Radio Astronomy (1st ed.; New York: McGraw-Hill)

Manchester, R. N. 1972, "Pulsar Rotation and Dispersion Measures and the Galactic Magnetic Field", ApJ, 172, 43

O'Donnell, M., Jaynes, E. T., & Miller, J. G. 1981, "Kramers-Kronig relationship between ultrasonic attenuation and phase velocity", J. Acoust. Soc. Am., 69, 696

Robishaw, T. 2008, "Magnetic fields near and far: Galactic and extragalactic single-dish radio observations of the Zeeman effect", Ph.D. Thesis, University of California, Berkeley

Robishaw, T., & Heiles, C. 2009, "On Measuring Accurate 21 cm Line Profiles with the Robert C. Byrd Green Bank Telescope", PASP, 121, 272